Submitted to
Annals of Physics

LBL-2154
Preprint

c. 1

NUMERICAL EVALUATION OF THE $1S_{\frac{1}{2}}$-STATE RADIATIVE LEVEL SHIFT

Peter J. Mohr

September 12, 1973

Prepared for the U. S. Atomic Energy Commission
under Contract W-7405-ENG-48

DISCLAIMER

NUMERICAL EVALUATION OF THE $1S_{\frac{1}{2}}$-STATE RADIATIVE LEVEL SHIFT*†

Peter J. Mohr

Lawrence Berkeley Laboratory
University of California
Berkeley, California 94720

September 12, 1973

* This work was supported in part by the U. S. Atomic Energy Commission and in part by the Air Force Office of Scientific Research, Office of Aerospace Research, United States Air Force, under Grant No. AF-AFOSR-68-1471.

† Based on a dissertation submitted to the University of California at Berkeley as partial fulfillment of the requirements for the degree of Doctor of Philosophy.

$1S_{\frac{1}{2}}$-STATE RADIATIVE LEVEL SHIFT

Peter J. Mohr

Lawrence Berkeley Laboratory
University of California
Berkeley, California 94720

ABSTRACT

The one-photon self-energy radiative level shift for an electron in a Coulomb potential is evaluated numerically for the $1S_{\frac{1}{2}}$ state. The evaluation is done for values of the nuclear charge $Z = 10,20,\cdots,110$. The errors in the values obtained are estimated to be less than 0.1%. The results are compared with the results of previous calculations. The evaluation is based on the expressions given in the preceding paper.

I. INTRODUCTION

In the preceding paper [1], the one-photon self-energy radiative level shift is expressed in a form suitable for direct numerical evaluation by a computer. In this paper, we describe the numerical evaluation for the case of the $1S_{\frac{1}{2}}$ state, for $Z = 10,20,\cdots,110$.

In Sec. II the numerical evaluation of ΔE_L is described. Values associated with ΔE_{HA} are given in Sec. III. Evaluation of the remainder ΔE_{HB} is described in Sec. IV. In Sec. V the results are summarized and compared with the results of previous calculations. Algorithms used to evaluate the special functions which arise in the calculation are described in appendices.

The value used for α^{-1} is 137.03602. The numerical calculations were done with the CDC 7600 computer at the Lawrence Berkeley Laboratory.

II. NUMERICAL EVALUATION OF THE LOW-ENERGY PART ΔE_L

We consider the numerical evaluation of $\mathrm{Re}(\Delta E_L)$ with the aid of (3.14) of I. In the case of the $1S_{\frac{1}{2}}$ state, specification of the principal value of the integral over z is not necessary, because there is no bound-state pole in the integrand in the interval $(0,E_n)$; ΔE_L is then real. We introduce new variables of integration in the expression (3.14) of I:

$$t = 1 - \frac{z}{E_n} ; \begin{cases} y = 2\gamma x_1 ; \quad r = \dfrac{x_2}{x_1} & \text{for } x_2 < x_1 \\ y = 2\gamma x_2 ; \quad r = \dfrac{x_1}{x_2} & \text{for } x_2 \geq x_1 . \end{cases} \tag{2.1}$$

In (2.1), $\gamma = Z\alpha$ and $E_n = (1 - \gamma^2)^{\frac{1}{2}}$. Employing these variables, and noting that the integrand is symmetric under interchange of x_2 and x_1, we have

$$\Delta E_L = \frac{\alpha}{\pi}\left[E_n + \int_0^1 dt \int_0^\infty dy \int_0^1 dr\, S(r,y,t,\gamma)\right] \quad (2.2)$$

where

$$S(r,y,t,\gamma) = -\frac{2E_n{}^2(2\gamma)^{-3}}{\Gamma(3-2\delta)}\, t r^{2-\delta}\, y^{5-2\delta}\, e^{-y}\, e^{\frac{1}{2}(1-r)y} \sum_{\kappa=1}^{\infty} T_\kappa(r,y,t,\gamma) \quad (2.3)$$

and where

$$T_\kappa(r,y,t,\gamma) = \sum_{\substack{\text{signs}\\ \text{of } \kappa}} \Bigg\{ (1 - E_n)\, G_\kappa{}^{11}(ru,u,z)|\kappa| \times \left[j'_{|\kappa+\frac{1}{2}|-\frac{1}{2}}(rv)\, j'_{|\kappa+\frac{1}{2}|-\frac{1}{2}}(v) + \frac{\kappa^2 - 1}{y_2 y_1}\, j_{|\kappa+\frac{1}{2}|-\frac{1}{2}}(rv)\, j_{|\kappa+\frac{1}{2}|-\frac{1}{2}}(v) \right]$$

$$- \gamma\, G_\kappa{}^{12}(ru,u,z)\kappa\, j'_{|\kappa+\frac{1}{2}|-\frac{1}{2}}(rv)\, j_{|\kappa-\frac{1}{2}|-\frac{1}{2}}(v)$$

$$- \gamma\, G_\kappa{}^{21}(ru,u,z)\kappa\, j_{|\kappa-\frac{1}{2}|-\frac{1}{2}}(rv)\, j'_{|\kappa+\frac{1}{2}|-\frac{1}{2}}(v)$$

$$+ (1 + E_n)\, G_\kappa{}^{22}(ru,u,z)|\kappa|\, j_{|\kappa-\frac{1}{2}|-\frac{1}{2}}(rv)\, j_{|\kappa-\frac{1}{2}|-\frac{1}{2}}(v) \Bigg\}; \quad (2.4)$$

$$\delta = 1 - E_n; \quad u = y/(2\gamma); \quad z = E_n(1 - t); \quad v = E_n t y/(2\gamma).$$

The expression which appears in (2.2) is in a form suitable for direct numerical evaluation by a computer. We shall first briefly outline the method we use, and then give a detailed description of each step. The triple integral which appears in (2.2) is evaluated by Gaussian quadrature. For certain values of $Z\alpha$, the multiple integral is evaluated three times. In each successive evaluation, the number of integration points in each dimension is increased. In this way, a convergent sequence of approximations to the integral is obtained. The integrand is in the form of an infinite sum over κ. This sum is evaluated for each set of values of the integration variables needed for the numerical evaluation of the multiple integral. The most significant contribution to the sum comes from terms for which $|\kappa| \lesssim rv$, where rv is the smaller of the arguments of the spherical Bessel functions. For $|\kappa| \gtrsim rv$, the terms in the sum approach zero rapidly as $|\kappa|$ increases. The spherical Bessel functions and radial Green's functions which appear in the individual terms of the sum are evaluated by algorithms which are described in Appendices B and D.

We first examine the sum over κ to establish the nature of its convergence. The asymptotic behavior of $T_\kappa(r,y,t,\gamma)$ as $\kappa \to \infty$ is found from the asymptotic behavior, shown in (A.5), of the radial Green's functions and from the asymptotic behavior of j_ℓ and j'_ℓ as $\ell \to \infty$:

$$j_\ell(x) \sim \frac{\ell!}{(2\ell+1)!}(2x)^\ell; \quad j'_\ell(x) \sim \frac{\ell}{x}\frac{\ell!}{(2\ell+1)!}(2x)^\ell. \quad (2.5)$$

We have

$$T_\kappa(r,y,t,\gamma) \sim A_\kappa(r,y,t,\gamma) = (1 - E_n)[\gamma + (1 + E_n - E_n t)u]$$

$$r^{-3}\, u^{-2}\, v^{-4}\, \kappa^2 \left[\frac{\kappa!}{(2\kappa)!}\right]^2 (2rv)^{2\kappa} \qquad (2.6)$$

as $\kappa \to \infty$. We obtain an indication of the rate of convergence of the sum over κ in (2.3) by considering the remainder

$$R_N = \sum_{\kappa=N+1}^{\infty} A_\kappa \quad . \qquad (2.7)$$

We find

$$\lim_{N\to\infty} \frac{R_N}{\left(\frac{e}{2}\frac{rv}{N}\right)^{2N}} = C \qquad (2.8)$$

where C is a constant independent of N. The above expression indicates the nature of the convergence of the partial sums

$$S_N = \sum_{\kappa=1}^{N} T_\kappa \qquad (2.9)$$

when N is so large that the terms T_κ, $\kappa > N$, are well approximated by the asymptotic forms A_κ. Actually, the partial sums are often close to the limit before N is sufficiently large for the asymptotic form to be a good approximation. The rapid convergence arises as follows. For $\ell > x$, the asymptotic forms in (2.5) are good approximations for the corresponding functions. For such ℓ, it is evident from the asymptotic forms that these functions decrease rapidly as ℓ increases. On the other hand, the other factors in T_κ are

relatively slowly varying as κ increases. Therefore, for κ greater than the smaller of the arguments of the Bessel functions, T_κ decreases rapidly as κ increases, and the partial sums S_N converge rapidly. The behavior of T_κ as a function of κ, for some values of the other parameters, is illustrated in Fig. 1. In the numerical computation of $S(r,y,t,\gamma)$, we terminate the sum over κ at $\kappa = N$ when both of the following conditions are met:

$$|T_{N+1}| < 10^{-15} \left|\sum_{\kappa=1}^{N} T_\kappa\right| ; \qquad N > rv \quad . \qquad (2.10)$$

We now describe the procedure we use for evaluating $S(r,y,t,\gamma)$. The evaluation is performed by a subroutine which, given a value for each of the arguments r, y, t, and γ, computes the value of $S(r,y,t,\gamma)$. First, within the subroutine, a number L

$$L = 2rv + 25 \qquad (2.11)$$

is computed. We find empirically that this number is always larger, and not excessively larger, than the smallest N which satisfies (2.10). The Bessel functions and their derivatives which appear in (2.4), with indices in the range 0 to L, are computed with the method described in Appendix B and stored in arrays. Then the sum over κ is performed. The radial Green's functions are evaluated as described in Appendix D. The summation over κ is terminated at $\kappa = N$, where N is the smallest number which satisfies the conditions in (2.10). Finally, the sum is multiplied by the remaining factors which appear in (2.3). The evaluation of the gamma function is described in Appendix F.

With values for $S(r,y,t,\gamma)$ available, we numerically evaluate the integrals in (2.2). The integrals are done by repeated one-dimensional Gaussian quadrature with new variables of integration which are defined in subsequent discussion. Integrals evaluated numerically over the interval $(0,1)$ are done, with the appropriate linear mapping to the interval $(-1,1)$, by Gauss-Legendre quadrature; integrals evaluated numerically over the interval $(0,\infty)$ are done by Gauss-Laguerre quadrature [2]. We designed the integration scheme to give the result correctly to 11 significant figures when $Z = 10$. The corresponding accuracy in the physically interesting part of the result is much less, for the following reason. The low-energy part ΔE_L is of order 1 [see (3.10) of I], while the renormalized self energy is well known to be of order $(Z\alpha)^4 \ln(Z\alpha)^{-2}$. Hence, in the worst case that we consider here, i.e., $Z = 10$, the physically interesting part of the number we compute is smaller than the number itself by a factor of order $(10\alpha)^4 \approx 3 \times 10^{-5}$.

We choose new variables of integration to be used in evaluating the integrals over r and y. In order to motivate our choice, we consider a simple function which exhibits the qualitative features of the dependence of $S(r,y,t,\gamma)$ on its variables. To find such a function, we recall that the main contribution to the sum $S(r,y,t,\gamma)$ comes from values of κ for which $|\kappa| < rv < ru$. Therefore, we expect that the behavior of the sum is qualitatively reproduced by the expression obtained if the radial Green's functions are replaced by their asymptotic forms, for $ru \gg |\kappa|$, which appear in (A.3). Taking the last term in (2.4) as a typical term in T_κ, making the above-mentioned replacement for the radial Green's functions, performing the sum over κ, and replacing the relatively slowly varying

factors by 1, we obtain

$$S(r,y,t,\gamma) \sim e^{-y} e^{-\frac{1}{2}(\frac{c}{\gamma}-1)(1-r)y} \frac{\sin[(1-r)v]}{(1-r)} \tag{2.12}$$

where $c = (1 - z^2)^{\frac{1}{2}}$, $\mathrm{Re}(c) > 0$. Here, the symbol $\sim$ means the functions on either side are qualitatively similar in their dependence on the variables. The factor $(\frac{c}{\gamma} - 1)$ in the exponent is positive for the range of values of the energy z under consideration.

We now consider the integral

$$S_1(y,t,\gamma) = \int_0^1 dr\, S(r,y,t,\gamma) . \tag{2.13}$$

We note, from (2.12), that the qualitative r dependence of the integrand is

$$e^{-q(1-r)} \frac{\sin[\theta q(1-r)]}{(1-r)} \tag{2.14}$$

where

$$q = \tfrac{1}{2}(\tfrac{c}{\gamma} - 1)y , \qquad 0 < q < \infty ;$$
$$0 < \theta < \left(\frac{1+\gamma}{1-\gamma}\right)^{\frac{1}{2}} . \tag{2.15}$$

For $Z \leq 110$, we have $\theta < \pi$. For q large, the sine function in (2.14) oscillates rapidly as r varies, but the oscillations are strongly damped by the exponential. To numerically evaluate the integral in (2.13), we employ the following prescription:

for $0 < q \leq 10$

$$S_1(y,t,\gamma) = \int_0^1 dx\, 2x\, S(x^2,y,t,\gamma)\,, \qquad N = [q] + 9\,;$$

for $10 < q \leq 30$

$$S_1(y,t,\gamma) = \int_0^1 dx\, S(x,y,t,\gamma)\,, \qquad N = \min([0.4q] + 8, 18)\,;$$

for $30 < q \leq 100$

$$S_1(y,t,\gamma) = \int_0^1 dx\, \frac{30}{q}\, S\left(1 - \frac{30}{q}\, x, y, t, \gamma\right) + \epsilon\,, \qquad N = 18\,;$$

for $q > 100$

$$S_1(y,t,\gamma) = \int_0^\infty dx\, \frac{1}{q}\, \bar{S}\left(1 - \frac{x}{q}, y, t, \gamma\right)\,, \qquad N = 8\,; \tag{2.16}$$

where N is the number of integration points used to evaluate the integral, $\bar{S}$ is given by

$$\bar{S}(r,y,t,\gamma) = \begin{cases} S(r,y,t,\gamma)\,, & 0 < r < 1 \\ 0\,, & r \leq 0\,; \end{cases} \tag{2.17}$$

and ϵ is given by

$$\epsilon = \int_1^{\frac{q}{30}} dx\, \frac{30}{q}\, S\left(1 - \frac{30}{q}\, x, y, t, \gamma\right)$$

$$\approx \int_1^{\frac{q}{30}} dx\, e^{-30x}\, e^{-y} \approx 3 \times 10^{-15}\, e^{-y}\,. \tag{2.18}$$

The contribution of ϵ in (2.16) is neglected. We arrived at the above prescription in the following way. We examined the integral numerically for $\gamma = 10\alpha$ and sample values of y and t which cover the range of numerical values given for these variables when the integrals over y and t are evaluated. For each fixed value of y and t, we tried various variables of integration in the integral over r, and for each variable of integration, we tried various numbers of points in the integration formula. A choice of integration variable and number of integration points was considered acceptable if the resulting value for the integral was correct to approximately 11 places beyond the decimal point, and the rate of convergence was good. The correctness of the result was judged by varying the number of points in the integration formula and observing the degree of stability of the corresponding values for the integral. By good rate of convergence for the integral, we mean one for which increasing the number of integration points by two, decreases the error in the result by approximately a factor of 10.

We next consider the integral

$$S_2(t,\gamma) = \int_0^\infty dy\, S_1(y,t,\gamma)\,. \tag{2.19}$$

The dominant y dependence of the integrand is simply e^{-y}. The method we use to numerically evaluate the integral in (2.19) is as follows:

$$S_2(t,r) = S_{21}(t,r) + S_{22}(t,r) + S_{23}(t,r) ;$$

$$S_{21}(t,r) = \int_0^1 dx\, S_1(x,t,r) , \qquad N = 14 ;$$

$$S_{22}(t,r) = \int_0^1 dx\, 4S_1(1 + 4x,t,r) , \qquad N = 12 ;$$

$$S_{23}(t,r) = \int_0^\infty dx\, S_1(5 + x,t,r) , \qquad N = 6 . \qquad (2.20)$$

The number N is the number of integration points used to evaluate the integral. We arrived at this method of evaluation by examining the integral in (2.19) for $r = 10\alpha$ and sample values for t. For each value of t, we tried various variables of integration and numbers of integration points to evaluate the integral. In choosing a method, we applied the same criterion of acceptability as in the integration over r.

We finally consider the integral over t

$$S_3(r) = \int_0^1 dt\, S_2(t,r) . \qquad (2.21)$$

The most significant feature of the integrand in (2.21) is the presence of the bound-state poles near t = 0. This integral is numerically evaluated as follows:

$$S_3(r) = S_{31}(r) + S_{32}(r) ;$$

$$S_{31}(r) = \int_0^1 dx\, 0.3x^2\, S_2(0.1x^3,r) , \qquad N = 14 ;$$

$$S_{32}(r) = \int_0^1 dx\, 2.7x^2\, S_2(0.1 + 0.9x^3,r) , \qquad N = 10 . \qquad (2.22)$$

The number N is again the number of integration points used in the numerical evaluation of each integral. We arrived at this method by using the same approach as was used in the preceding integrations.

For Z = 10, 20, 30, 50, 70, 90, and 110, we numerically evaluated the integral in (2.2) three times, employing the variables displayed in Eqs. (2.16), (2.20), and (2.22). In the first evaluation, the number of integration points used to evaluate each integral was two less than the value given for N for that integral. In the second evaluation, the number of integration points used to evaluate each integral was equal to the value given for N for that integral. In the third evaluation, the number of integration points was two greater than the value given for N. For Z = 40, 60, 80, and 100, the integrals were evaluated once with the number of integration points equal to the values given for N. The results of these evaluations are listed in Table I. Values for $f_L(Z\alpha)$, which is defined in (3.18) of I, corresponding to the numbers obtained for $S_3(Z\alpha)$ are also listed in that table.

Table I. Computed values for $S_3(Z\alpha)$ and $f_L(Z\alpha)$

Z	$S_3(Z\alpha)$	$f_L(Z\alpha)$
10	0.492604558261	5.885057461
	0.492604558212	5.885055755
	0.492604558219	5.885055985
20	0.471522661337	4.399376065
	0.471522662028	4.399377589
	0.471522662053	4.399377644
30	0.438918124592	3.635616766
	0.438918122718	3.635615950
	0.438918122834	3.635616000
40	0.397217582472	3.157389794
50	0.348910859260	2.832339685
	0.348910857608	2.832339592
	0.348910857653	2.832339594
60	0.296473044488	2.604438382
70	0.242325295399	2.446696882
	0.242325282906	2.446696699
	0.242325282216	2.446696689
80	0.188809276812	2.346786654
90	0.138167108750	2.302805682
	0.138167073328	2.302805492
	0.138167073750	2.302805494
100	0.092524835161	2.325000983
110	0.053885535012	2.447660167
	0.053885561168	2.447660230
	0.053885562857	2.447660234

If, in the sets of three values for $S_3(Z\alpha)$ obtained for $Z = 10, 20, 30, 50, 70, 90,$ and 110, the difference between the second and third numbers is taken as an approximate measure of the error in the second number, then the order of magnitude of that error is a fairly slowly varying function of Z. In view of this, one can infer the magnitude of error in the values of $S_3(Z\alpha)$ for $Z = 40, 60, 80,$ and 100 by interpolation. We note that the errors, as defined above, in the values for $S_3(Z\alpha)$ increase as Z increases. This is to be expected as the integration scheme is designed for $Z = 10$. On the other hand, the errors in the values for $f_L(Z\alpha)$ decrease as Z increases because the effect in $f_L(Z\alpha)$ of the error in $S_3(Z\alpha)$ becomes less important.

As a test against errors in algebra or programming in the evaluation of the low-energy part, we consider the behavior of the numbers in Table I in the limit $Z\alpha \to 0$. From (3.10) of I, it follows that

$$\lim_{Z\alpha\to 0} S_3(Z\alpha) = \frac{1}{2} . \tag{2.23}$$

This condition, which is not very stringent, appears to be satisfied by the calculated numbers. The behavior of $f_L(Z\alpha)$ provides a better test. From (6.3) of I, we have

$$\begin{aligned} f_L(Z\alpha) &= F(Z\alpha) - f_{HA}(Z\alpha) - f_{HB}(Z\alpha) \\ &= \frac{4}{3}\ell n(Z\alpha)^{-2} - 1.5546\cdots + \mathcal{O}(Z\alpha) . \end{aligned} \tag{2.24}$$

The second line in (2.24) follows from the known behavior of $F(Z\alpha)$ for small $Z\alpha$ given in (1.2) of I, and from the values for $f_{HA}(0)$

and $f_{HB}(0)$ given in (3.5) and (4.23) respectively. We check for this behavior by plotting values of the function

$$f_L(Z\alpha) - \frac{4}{3}\,\ell n(Z\alpha)^{-2} \qquad (2.25)$$

and the limit point in Fig. 2. The calculated points in this figure are consistent with the limit point -1.5546. We note that a deviation of 10^{-5} in the value for $S_3(Z\alpha)$ at $Z = 10$ would produce a deviation of 0.35 in $f_L(Z\alpha)$ which would be enough to destroy the consistency in Fig. 2.

III. THE FUNCTION $f_{HA}(Z\alpha)$

We consider the function $f_{HA}{}^1(Z\alpha)$ which appears in (4.15) of I. For the $1S_{\frac{1}{2}}$ state, we have

$$E_{1S}{}^2 = 1 - (Z\alpha)^2 \ ,$$

$$\langle V \rangle = \frac{-(Z\alpha)^2}{[1 - (Z\alpha)^2]^{\frac{1}{2}}} \ , \qquad (3.1)$$

$$\left\langle \left(1 - \frac{\beta}{E_{1S}}\right) V \right\rangle = 0 \ .$$

Numerical values for $f_{HA}{}^1(Z\alpha)$ are listed in Table II. We note from the formula for $f_{HA}{}^1(Z\alpha)$ that

$$\lim_{Z\alpha \to 0} f_{HA}{}^1(Z\alpha) = -\frac{7}{12} - \frac{1}{4}\,\ell n\ 2 \ . \qquad (3.2)$$

We next consider evaluation of the functions h_i, $i = 1,2,3,4$. These functions are given as one-dimensional integrals in (4.23) of I. The functions g_i and $(Vg)_i$, $i = 1,2$, which appear in those formulas, are given explicitly for the $1S_{\frac{1}{2}}$ state in the appendix of I. The

integrals in (4.23) of I were evaluated by Gaussian quadrature with new variables of integration x given by

$$p = (Z\alpha)\frac{1 - x^2}{x^2} \qquad \text{in } h_1, h_2 \ ;$$

$$p = (Z\alpha)\frac{1 - x^3}{x^3} \qquad \text{in } h_3, h_4 \ . \qquad (3.3)$$

We used a 60-point Gauss-Legendre formula. The numerical error in the h's with this method of evaluation, as determined by observing the convergence in the values for the integrals as the number of integration points is increased, is of the order of 10^{-12} or less for $10 \le Z \le 110$. The results of this evaluation are listed in Table II. The limits of $h_i(Z\alpha)$, $i = 1,2,3,4$, as $Z\alpha \to 0$, are

$$h_1(0) = \frac{31}{420} \ ,$$

$$h_2(0) = \frac{5}{4}\,\ell n\ 2 - \frac{118}{105} \ ,$$

$$h_3(0) = 9\,\ell n\ 2 - \frac{31}{5} \ , \qquad (3.4)$$

$$h_4(0) = 8 - 12\,\ell n\ 2 \ .$$

Values for the function $f_{HA}(Z\alpha)$, which is defined in (4.25) of I, are listed in Table II. From (3.2) and (3.4), we have

$$\lim_{Z\alpha \to 0} f_{HA}(Z\alpha) = \frac{1}{6} - 2\,\ell n\ 2 \ . \qquad (3.5)$$

Table II. The results of numerical evaluation of f_{HA}^{1}, h_1, h_2, h_3, h_4, and the total f_{HA}. All figures shown are significant.

Z	$f_{HA}^{1}(Z\alpha)$	$h_1(Z\alpha)$	$h_2(Z\alpha)$	$h_3(Z\alpha)$	$h_4(Z\alpha)$	$f_{HA}(Z\alpha)$
10	-0.759762	0.061029	-0.235254	0.041051	-0.308422	-1.201358
20	-0.769348	0.047569	-0.219782	0.045286	-0.303368	-1.199643
30	-0.785874	0.033259	-0.208071	0.050676	-0.301391	-1.211401
40	-0.810250	0.017768	-0.198607	0.057061	-0.301606	-1.235634
50	-0.843934	0.000742	-0.190326	0.064314	-0.303269	-1.272473
60	-0.889193	-0.018187	-0.182321	0.072286	-0.305666	-1.323081
70	-0.949575	-0.039426	-0.173684	0.080762	-0.308012	-1.389936
80	-1.030831	-0.063471	-0.163350	0.089399	-0.309339	-1.477591
90	-1.142851	-0.091023	-0.149890	0.097638	-0.308314	-1.594440
100	-1.304309	-0.123305	-0.131106	0.104522	-0.302901	-1.757100
110	-1.555971	-0.163032	-0.103036	0.108286	-0.289584	-2.003337

IV. NUMERICAL EVALUATION OF THE REMAINDER ΔE_{HB}

In the expression for ΔE_{HB} in (5.7) of I, we introduce the variable of integration t, where $z = i(t^{-1} - t)/2$ on the positive imaginary z-axis and $z = -i(t^{-1} - t)/2$ on the negative imaginary z-axis. We also introduce the variables y and r defined in (2.1). Then, for the function f_{HB} defined in (5.10) of I, we have

$$f_{HB}(\gamma) = \int_0^1 dt \int_0^\infty dy \int_0^1 dr\, S(r,y,t,\gamma) \tag{4.1}$$

where

$$S(r,y,t,\gamma) = \frac{8(2\gamma)^{-7}}{\Gamma(3-2\delta)} (t^{-2}+1)\, r^{2-\delta}\, y^{5-2\delta}\, e^{-y}\, e^{\frac{1}{2}(1-r)y} \times \sum_{\kappa=1}^{\infty} T_\kappa(r,y,t,\gamma) \tag{4.2}$$

and where

$$T_\kappa(r,y,t,\gamma) = -\sum_{\substack{\text{signs}\\ \text{of } \kappa}} |\kappa|\, \mathrm{Re}\Big([u + iE_n]\{[(1+E_n)\, G^{11}_{B,\kappa} - \gamma G^{12}_{B,\kappa} - \gamma G^{21}_{B,\kappa} + (1-E_n) G^{22}_{B,\kappa}]\, j_{|\kappa+\frac{1}{2}|-\frac{1}{2}}\, h^{(1)}_{|\kappa+\frac{1}{2}|-\frac{1}{2}} - [3(1-E_n)\, G^{11}_{B,\kappa} - \gamma G^{12}_{B,\kappa} - \gamma G^{21}_{B,\kappa} + 3(1+E_n) G^{22}_{B,\kappa}]\, j_{|\kappa-\frac{1}{2}|-\frac{1}{2}}\, h^{(1)}_{|\kappa-\frac{1}{2}|-\frac{1}{2}} + (1-E_n)\, G^{11}_{B,\kappa} \times 4\frac{\kappa+1}{|2\kappa+1|} [j_{|\kappa+\frac{1}{2}|-\frac{3}{2}}\, h^{(1)}_{|\kappa+\frac{1}{2}|-\frac{3}{2}} - j_{|\kappa+\frac{1}{2}|+\frac{1}{2}}\, h^{(1)}_{|\kappa+\frac{1}{2}|+\frac{1}{2}}]\} \Big) \tag{4.3}$$

The functions G_B are defined in (5.5) of I. The arguments of the functions G_B, j, and $h^{(1)}$ in (4.3) are given by

$$G^{ij}_{B,\kappa} = G^{ij}_{B,\kappa}(ru,u,w) \ ,$$

$$j_\kappa = j_\kappa\big((w - E_n)ru\big) \ , \qquad (4.4)$$

$$h^{(1)}_\kappa = h^{(1)}_\kappa\big((w - E_n)u\big) \ ,$$

$$u = y/(2\gamma) \ ; \qquad w = i(t^{-1} - t)/2 \ .$$

The numerical evaluation of ΔE_{HB} is similar to the evaluation of ΔE_L. The integration in (4.1) is performed by repeated Gaussian quadrature. The function $S(r,y,t,\gamma)$ is computed with the aid of (4.2); the truncation of the sum over κ is discussed below. The numerical evaluation of the spherical Bessel functions, spherical Hankel functions, and radial Green's functions which appear in (4.3) is described in Appendices C and E.

We now examine the convergence of the sum over κ in (4.2). For $\kappa \to +\infty$, we have

$$G^{11}_{B,\kappa}(ry,y,z) = \frac{r^{\kappa-1}}{2\kappa y^2}\left[\tfrac{1}{2}\gamma(1 - r) + \mathcal{O}(\tfrac{1}{\kappa})\right] \ ,$$

$$G^{12}_{B,\kappa}(ry,y,z) = \frac{r^{\kappa-1}}{2\kappa y^2}\left[\mathcal{O}(\tfrac{1}{\kappa})\right] \ ,$$

$$G^{21}_{B,\kappa}(ry,y,z) = \frac{r^{\kappa-1}}{2\kappa y^2}\left[2\gamma z(1 - r)y - \gamma^2 \ell n\ r + \mathcal{O}(\tfrac{1}{\kappa})\right] \ ,$$

Equation (4.5) continued next page

Equation (4.5) continued

$$G^{22}_{B,\kappa}(ry,y,z) = \frac{r^{\kappa-1}}{2\kappa y^2}\left[\tfrac{1}{2}\gamma(1 - \tfrac{1}{r}) + \mathcal{O}(\tfrac{1}{\kappa})\right] \ ,$$

$$G^{11}_{B,-\kappa}(ry,y,z) = \frac{r^{\kappa-1}}{2\kappa y^2}\left[\tfrac{1}{2}\gamma(1 - \tfrac{1}{r}) + \mathcal{O}(\tfrac{1}{\kappa})\right] \ ,$$

$$G^{12}_{B,-\kappa}(ry,y,z) = -\frac{r^{\kappa-1}}{2\kappa y^2}\left[2\gamma z(1 - r)y - \gamma^2 \ell n\ r + \mathcal{O}(\tfrac{1}{\kappa})\right] \ ,$$

$$G^{21}_{B,-\kappa}(ry,y,z) = \frac{r^{\kappa-1}}{2\kappa y^2}\left[\mathcal{O}(\tfrac{1}{\kappa})\right] \ ,$$

$$G^{22}_{B,-\kappa}(ry,y,z) = \frac{r^{\kappa-1}}{2\kappa y^2}\left[\tfrac{1}{2}\gamma(1 - r) + \mathcal{O}(\tfrac{1}{\kappa})\right] \qquad (4.5)$$

and

$$j_\kappa(ry)\, h^{(1)}_\kappa(y) = \frac{r^\kappa}{2\kappa i y}\left[1 + \mathcal{O}(\tfrac{1}{\kappa})\right] . \qquad (4.6)$$

Hence, for fixed r, y, t, and γ,

$$T_\kappa(r,y,t,\gamma) = 2\gamma^4 \frac{r^{2\kappa-2}}{\kappa y^3}(1 - r)$$

$$\times\left[(1 + E_n)\frac{1 - r^2}{r} + (1 - E_n)\frac{1 - r^4}{r^2} - 2\gamma^2 \ell n\ r + \mathcal{O}(\tfrac{1}{\kappa})\right] \qquad (4.7)$$

as $\kappa \to \infty$. We define a function $P_\kappa(r,y,t,\gamma)$ by writing

$$T_\kappa(r,y,t,\gamma) = \frac{r^{2\kappa}}{\kappa} P_\kappa(r,y,t,\gamma) . \qquad (4.8)$$

In order to obtain an approximation for the remainder R_N which is left if the sum over κ in (4.2)is truncated at $\kappa = N$, we assume that for $\kappa \geq 1.5$ cu , where $c = (1 - w^2)^{\frac{1}{2}}$ and $Re(c) > 0$, the function P_κ, as a function of κ, is sufficiently slowly varying compared to $(r^{2\kappa})/\kappa$ that the following approximation is justified:

$$R_N = \sum_{\kappa=N+1}^{\infty} T_\kappa \simeq P_{N+1} \sum_{\kappa=N+1}^{\infty} \frac{r^{2\kappa}}{\kappa} \quad . \tag{4.9}$$

This assumption is suggested by the form of the expression in (4.7) together with a numerical examination of the terms in the sum in (4.2) for various values of the parameters. From (4.9), we obtain

$$|R_N| \lesssim \frac{1}{1 - r^2} |T_{N+1}| \quad . \tag{4.10}$$

The sum over κ in (4.2) is thus truncated at $\kappa = N$, where N is the smallest number which is greater than 3, greater than or equal to 1.5 cu, and large enough that the magnitude of the absolute contribution of the remainder, as estimated by (4.10), to the sum S is less than 10^{-4}. The validity of this error approximation was tested by evaluating the sum S with the cutoff described above, and then re-evaluating the sum with the error bound of 10^{-4} replaced by an error bound of 10^{-6}. The two values for the sum were then compared. The evaluation and comparison was made for all combinations of the values $r = 0.1, 0.5, 0.9$, $y = 0.1, 1, 10$, $t = 0.1, 0.5, 0.9$, and $\gamma = 10/137, 110/137$, and for the values $(r,y,t,\gamma) = (0.99, 10, 0.1, 110/137)$, $(0.999, 10, 0.1, 110/137)$, $(0.99, 1, 0.1, 10/137)$, $(0.999, 1, 0.1, 10/137)$, $(0.99, 10, 0.9, 10/137)$, and $(0.999, 10, 0.9, 10/137)$. In all cases, the magnitude

of the difference between the two values for S is less than 10^{-4}. The validity of the error approximation was further tested by varying the error bound in some of the final evaluations of ΔE_{HB}.

In the evaluation of the sum S, the products of Bessel functions which appear in (4.3) are evaluated recursively, as described in Appendix C, before the sum over κ in (4.2) is performed. Therefore, we need a preliminary moderate overestimate N_0 for the number of Bessel functions which are needed to evaluate the sum to the desired accuracy. The value we employ for this purpose, for specified values of r, y, t, and γ, is given by

$$N_0 = \max(N_1, N_2, 3) + 1 \tag{4.11}$$

where

$$N_1 = [1.5 \text{ cu}] \tag{4.12}$$

and

$$N_2 = \left[0.5 \frac{\ell n\left(\frac{1 - r^2}{10^4 \text{ B } P_\infty}\right)}{\ell n\ r} \right] + 3 \tag{4.13}$$

where B is the coefficient of the sum over κ in (4.2). If it is found, in a particular evaluation of S, that N_0 is too small, then the value of N_0 is increased by 10 and the evaluation of S is begun again.

A crude approximation for the function $S(r,y,t,\gamma)$, which serves to motivate our choice of new variables of integration in the numerical evaluation of the integral in (4.1), is obtained by replacing the radial Green's functions in (4.3) by their asymptotic

forms for large argument which appear in (A.3). Taking the first term in the curly brackets in (4.3) as a typical term, replacing the radial Green's functions in that term by the first terms in the corresponding asymptotic expansions, and performing the sum over κ, we obtain

$$S(r,y,t,\gamma) \sim e^{-y}\, e^{-\frac{1}{2}(\frac{1}{\gamma t}-1)(1-r)y} \quad . \tag{4.14}$$

In arriving at the expression in (4.14), we have set relatively slowly varying factors equal to 1. Two singular factors t^{-2} and $(1 - r)^{-1}$ which have been set equal to 1 in arriving at (4.14) are the result of the crude nature of the approximation. The behavior of S near $t = 0$ corresponds to the behavior of the integrand in (5.6) of I for large $|z|$. From the construction of ΔE_{HB} considered in I, it follows that S is integrable in this region. That S is integrable near $r = 1$ is seen by inspection of (4.7).

We next give the method that we use to numerically evaluate the integral in (4.1). The Gaussian integration formulas mentioned in Sec. II are used here. We employ the notation

$$S_1(y,t,\gamma) = \int_0^1 dr\, S(r,y,t,\gamma) \quad ,$$

$$S_{21}(t,\gamma) = \int_0^2 dy\, S_1(y,t,\gamma) \quad ,$$

$$S_{22}(t,\gamma) = \int_2^\infty dy\, S_1(y,t,\gamma) \quad ,$$

Equation (4.15) continued next page

Equation (4.15) continued

$$S_{3i}(\gamma) = \int_0^1 dt\, S_{2i}(t,\gamma) \quad , \qquad i = 1,2 \; ;$$

$$q = \tfrac{1}{2}(\tfrac{1}{\gamma t} - 1)y \quad . \tag{4.15}$$

Four regions, A, B, C, and D, in the space of the parameters r, y, t and $\gamma = Z\alpha$ are defined by

$$\begin{aligned} &\text{A:}\quad y < 2, \quad Z < 60 \; ; \\ &\text{B:}\quad y < 2, \quad Z \geq 60 \; ; \\ &\text{C:}\quad y > 2, \quad Z < 60 \; ; \\ &\text{D:}\quad y > 2, \quad Z \geq 60 \; . \end{aligned} \tag{4.16}$$

In the following, N_A, N_B, N_C, and N_D are the number of integration points used in the evaluation of the integrals with which they appear when the parameters are in the corresponding regions. The integral over r in (4.1) is evaluated as follows:

$$S_1(y,t,\gamma) = \int_0^1 dx\, 2x\, S(x^2,y,t,\gamma) \quad , \qquad 0 < q \leq 1 \; ;$$

$$S_1(y,t,\gamma) = \int_0^1 dx\, S(x,y,t,\gamma) \quad , \qquad 1 < q \leq 12 \; ;$$

$$S_1(y,t,\gamma) = \int_0^1 dx\, \frac{12}{q}\, S(1 - \frac{12}{q}\, x,y,t,\gamma) + \epsilon \quad , \qquad q > 12$$

(4.17)

where for all three integrals

$$N_A = N_C = N_D = 5 , \quad N_B = \begin{cases} 6 & \text{for } t \geq 0.2 \\ 8 & \text{for } t < 0.2 \end{cases} \tag{4.18}$$

and where

$$\epsilon = \int_1^{\frac{q}{12}} dx \, \frac{12}{q} \, S(1 - \tfrac{12}{q}x, y, t, r) \quad . \tag{4.19}$$

The contribution of ϵ to the value of the integral in (4.17) is neglected. In view of (4.14), an approximate overestimate for ϵ is given by

$$\epsilon \approx A(1 - \tfrac{12}{q}, y, t, r) \int_1^{\frac{q}{12}} dx \, e^{-12x} \, e^{-y}$$

$$\leq \frac{1}{12} S(1 - \tfrac{12}{q} x_0, y, t, r) \tag{4.20}$$

where $A(r,y,t,r)$ is the ratio of $S(r,y,t,r)$ to the term on the right side in (4.14), and x_0 is the largest value assigned to x in the numerical evaluation represented by the third equation in (4.17). We examined the corresponding values for S which occurred in the numerical integrations and found, based on the estimate in (4.20), that the magnitude of ϵ was always less than 4×10^{-4}, and in most cases it was much less than that value. We evaluate the integral over y in (4.1) in the following way:

$$S_{21}(t,r) = \int_0^1 dx \, 4x \, S_1(2x^2, t, r) ,$$

$$N_A = \begin{cases} 10 & \text{for } t \geq 0.5 \\ 12 & \text{for } t < 0.5 , \end{cases} \qquad N_B = \begin{cases} 8 & \text{for } t \geq 0.4 \\ 10 & \text{for } 0.1 \leq t < 0.4 \\ 12 & \text{for } t < 0.1 ; \end{cases}$$

$$S_{22}(t,r) = \int_0^\infty dx \, S_1(2 + x, t, r) ,$$

$$N_C = N_D = \begin{cases} 4 & \text{for } t > 0.5 \\ 3 & \text{for } t \leq 0.5 . \end{cases} \tag{4.21}$$

The integral over t in (4.1) is evaluated as follows:

$$S_{31}(r) = \int_0^1 dx \, 2x \, S_{21}(1 - x^2, r) , \quad N_A = 6 ; \tag{4.22}$$

$$S_{3i}(r) = \int_0^1 dx \, S_{2i}(x, r) , \qquad \begin{aligned} i = 1; \quad & N_B = 6 \\ i = 2; \quad & N_C = 4, \\ & N_D = 5 . \end{aligned}$$

The choices of variables of integration and numbers of integration points in the preceding discussion are the results of an effort to obtain a numerical value for the integrals in (4.1) with an error less than 5×10^{-4} in magnitude and with the use of a minimum amount of computer time. We arrived at the above scheme with an approach

analogous to the one used in the numerical evaluation of the low-energy part. The values for N_A, N_B, N_C, and N_D were determined by an examination of the integrals at the values $Z = 30$, 110, 50, and 110 respectively.

The results of the numerical integrations are given in Table III. In that table, where three values are given for a single point, the middle value is the result obtained with the above described method of integration; the upper value is the result of evaluating the integrals with a number of integration points in each integral which is one less than the number of integration points specified for that integral in the above method; the lower value is the result obtained with one extra integration point in each integral. The single values in that table are the results of evaluating the integrals with the method of integration described above, except that the value for S_{32} at $Z = 40$ is obtained with one extra integration point in each integral. Values for f_{HB}, obtained by adding the corresponding values for S_{31} and S_{32}, are also listed in Table III. We have given error limits with each value for f_{HB}. These are subjective estimates of the maximum uncertainty in the values, based on an examination of the behavior of the numbers within the groups of three values obtained for S_{31} and S_{32} for a given Z. For values of Z for which only one evaluation was made, the error limit was obtained by interpolating between the error limits for neighboring values of Z. The numbers marked with an asterisk in Table III are the values obtained by evaluating the integrals with the integration method described above, and with the error bound employed in truncating the sum over κ reduced to 10^{-5}. Comparison of these values with the corresponding unstarred values in

Table III. Computed values for $S_{31}(Z\alpha)$, $S_{32}(Z\alpha)$, and $f_{HB}(Z\alpha)$.

Z	$S_{31}(Z\alpha)$	$S_{32}(Z\alpha)$	$f_{HB}(Z\alpha)$
10	-0.007094	-0.027008	
	-0.007685	-0.020876	
	-0.007650	-0.022085	-0.030(2)
20	0.070451	-0.024465	0.046(1)
30	-0.155291	-0.025616	
	0.154183	-0.026785	
	0.154438	-0.026712	0.1277(5)
40	0.252596	-0.039257	0.2133(7)
50	0.359596	-0.052991	
	0.358150	-0.054137	
	0.357949	-0.053430	0.3045(8)
60	0.458330	-0.055898	0.4024(4)
70	0.552628	-0.041619	
	0.552438	-0.041645	
	0.552314	-0.041598	0.5107(4)
80	0.646615	-0.012562	0.6341(6)
90	0.752997	0.026850	
	0.752544	0.027536	
	0.752223	0.027442	0.7797(7)
100	0.888973	0.074809	0.9638(8)
110	1.092590	0.124257	
	1.091980	0.125498	
	1.091547	0.125506	1.2171(8)
30	0.154205*	-0.026737*	
110	1.092001*	0.125555*	

the table indicates that the method used to attain the desired accuracy in the sum over κ is effective.

As a check against errors in algebra or programming in the numerical evaluation of f_{HB}, we plot, in Fig. 3, the calculated values for $f_{HB}(Z\alpha)$ for $Z = 10, 20, 30, 40,$ and 50 and the limit point $f_{HB}(0)$. From (5.11) of I, we have

$$f_{HB}(0) = \frac{2}{3} \ell n\, 2 - \frac{5}{9} \cong -0.093457. \tag{4.23}$$

The calculated points appear to be consistent with the limit point.

V. CONCLUSION

The total value of the self-energy radiative level shift for the $1S_{\frac{1}{2}}$ state is given by

$$\Delta E_n = \frac{\alpha}{\pi} (Z\alpha)^4 F(Z\alpha)\, m_e c^2 \tag{5.1}$$

where

$$F(Z\alpha) = f_L(Z\alpha) + f_{HA}(Z\alpha) + f_{HB}(Z\alpha) \ . \tag{5.2}$$

Values for $F(Z\alpha)$ are given in Table IV. The numbers in parentheses in that table are error limits associated with f_{HB}, and are discussed near the end of Sec. IV. The calculated values for $F(Z\alpha)$ along with values for $F(Z\alpha)$ obtained from the results of previous calculations [3,4,5] are shown in Fig. 4.

For Z in the range 70-90, we compare the results of this calculation with the results, for a Coulomb potential, of Desiderio and Johnson [4]. In Table V we list the values they give (in Rydbergs), the corresponding values for $F(Z\alpha)$, and the values that we obtain for $F(Z\alpha)$. The agreement is good.

To compare our calculated values for $F(Z\alpha)$ to the known behavior of $F(Z\alpha)$ as $Z\alpha \to 0$, we consider the function

$$G(Z\alpha) = (Z\alpha)^{-2} [F(Z\alpha) - A_{40} - A_{41}\, \ell n (Z\alpha)^{-2} - A_{50}(Z\alpha)$$

$$- A_{61}(Z\alpha)^2\, \ell n (Z\alpha)^{-2} - A_{62}(Z\alpha)^2\, \ell n^2 (Z\alpha)^{-2}] \tag{5.3}$$

where the A_{ij} are the coefficients which appear in (1.2) of I. In view of that equation, we have

$$\lim_{Z\alpha \to 0} G(Z\alpha) = A_{60} \ . \tag{5.4}$$

Table IV. Values for $F(Z\alpha)$ obtained in this calculation.

Z	$F(Z\alpha)$
10	4.654(2)
20	3.246(1)
30	2.5519(5)
40	2.1351(7)
50	1.8644(8)
60	1.6838(4)
70	1.5675(4)
80	1.5032(6)
90	1.4880(7)
100	1.5317(8)
110	1.6614(8)

Table V. The results of the Desiderio and Johnson calculation for a Coulomb potential and the results of this calculation. The numbers in the third column are the Desiderio and Johnson results converted to our units and rounded to three figures. The numbers in the fourth column are our results rounded to three figures.

Z	Desiderio and Johnson[4] ΔE_n(Ry)	Desiderio and Johnson $F(Z\alpha)$	This calculation $F(Z\alpha)$
70	9.1	1.53	1.57
75	11.9	1.52	
80	15.0	1.48	1.50
85	19.1	1.48	
90	23.5	1.45	1.49

If there were a significant inconsistency between our calculated values for $F(Z\alpha)$ and the coefficients which appear in (5.3), except possibly for A_{61}, then $G(Z\alpha)$ would increase rapidly in magnitude as $Z\alpha \to 0$. We have plotted the values of $G(Z\alpha)$ corresponding to the calculated values of $F(Z\alpha)$ in Fig. 5. Inspection of the points in that figure suggests that $G(Z\alpha)$ approaches a constant as $Z\alpha \to 0$. We obtain an approximate value for that constant by fitting the function

$$G_A(Z\alpha) = \bar{A}_{60} + \bar{A}_{70}(Z\alpha) + \bar{A}_{71}(Z\alpha)\, \ell n(Z\alpha)^{-2} \qquad (5.5)$$

to the calculated values of $G(Z\alpha)$ at the points $Z = 10$, 20, and 30. There is some theoretical motivation for employing this function in making the fit. We thus obtain

$$\bar{A}_{60} = -31 \ . \qquad (5.6)$$

This value, taken as an approximation to A_{60}, has uncertainty associated with the errors in the values of the points used in making the fit and uncertainty associated with higher order terms in $G(Z\alpha)$ which are missing from $G_A(Z\alpha)$. Erickson and Yennie [6] and Erickson [3] have given the following estimates for A_{60}:

$$A_{60} = -\tfrac{4}{3}(19.08 \pm 5) \simeq -25.4 \pm 6.7 \qquad \text{(Ref. 6)} \ , \qquad (5.7)$$

$$A_{60} = -\tfrac{4}{3}(19.3435 \pm 0.5) \simeq -25.79 \pm 0.67 \qquad \text{(Ref. 3)} \ .$$

Our numerical values are reasonably consistent with the known behavior of $F(Z\alpha)$ for small $Z\alpha$ and with the values obtained by Desiderio and Johnson for Z near 80. For Z greater than 90, $F(Z\alpha)$ appears to increase rapidly. This is consistent with the result

of a preliminary investigation we have made which indicates that $F(Z\alpha) \to +\infty$ as $Z\alpha \to 1-$ [7]. This is not a surprising result for a pure Coulomb potential.

ACKNOWLEDGMENTS

I wish to thank Professor Eyvind H. Wichmann for his guidance and continued interest during the course of this work. Helpful conversations with Dr. James Daley, Mr. Miklos Gyulassy, Dr. Joseph V. Lepore, Dr. Robert J. Riddell, Jr., and Professor Charles Schwartz are gratefully acknowledged.

APPENDIX A

We list here asymptotic forms for the radial Green's functions defined in the appendix of I. We shall restrict our attention to the case in which $x_2 < x_1$ in $G_\kappa^{ij}(x_2,x_1,z)$. We give the asymptotic behavior in terms of new variables defined by

$$y = x_1 ; \qquad r = \frac{x_2}{x_1} . \tag{A.1}$$

The first limit of interest is for x_2 and $x_1 \gg |\kappa|$. The Whittaker functions have the following asymptotic forms, for α,β fixed, $\beta > 0$, $x > 0$ [8],

$$M_{\alpha,\beta}(x) = \frac{\Gamma(1+2\beta)}{\Gamma(\beta+\frac{1}{2}-\alpha)} e^{\frac{x}{2}} x^{-\alpha}\left[1 - \frac{(\beta+\frac{1}{2}+\alpha)(\beta-\frac{1}{2}-\alpha)}{x} + \mathcal{O}(\frac{1}{x^2})\right],$$

$$W_{\alpha,\beta}(x) = e^{\frac{x}{2}} x^{\alpha}\left[1 + \frac{(\beta+\frac{1}{2}-\alpha)(\beta-\frac{1}{2}+\alpha)}{x} + \mathcal{O}(\frac{1}{x^2})\right] \tag{A.2}$$

as $x \to \infty$. By $x^{\pm\alpha}$, we mean $e^{\pm\alpha \ell n\, x}$, $\ell n\, x$ real. From these expressions, we find

$$G_\kappa^{11}(ry,y,z) = (z+1)\, S\left\{1 + \frac{1+r}{2cry}\frac{r}{c} - \frac{1-r}{2cry}\left[\kappa(\kappa+1) - \frac{r^2}{c^2}\right] + \mathcal{O}(\frac{1}{y^2})\right\} ,$$

Equation (A.3) continued next page

Equation (A.3) continued

$$G_\kappa^{12}(ry,y,z) = -cS\left\{1 - \frac{1+r}{2cry}\kappa - \frac{1-r}{2cry}\left[\kappa^2 - \frac{r}{c}\left(1+\frac{r}{c}\right)\right] + \mathcal{O}(\frac{1}{y^2})\right\} ,$$

$$G_\kappa^{21}(ry,y,z) = cS\left\{1 + \frac{1+r}{2cry}\kappa - \frac{1-r}{2cry}\left[\kappa^2 + \frac{r}{c}\left(1-\frac{r}{c}\right)\right] + \mathcal{O}(\frac{1}{y^2})\right\} ,$$

$$G_\kappa^{22}(ry,y,z) = (z-1)\, S\left\{1 - \frac{1+r}{2cry}\frac{r}{c} - \frac{1-r}{2cry}\left[\kappa(\kappa-1) - \frac{r^2}{c^2}\right] + \mathcal{O}(\frac{1}{y^2})\right\} ,$$

$$S = \frac{r^{-\nu}}{2cry^2} e^{-(1-r)cy} . \tag{A.3}$$

The symbols ν, γ, and c are defined in (A.17) of I.

The second limit of interest is for $|\kappa| \gg x_1 > x_2$. For α,x fixed, $x > 0$, the Whittaker functions have the following asymptotic forms [8]

$$M_{\alpha,\beta}(x) = x^{\beta+\frac{1}{2}}\left[1 + \frac{\frac{1}{4}(\frac{x}{2})^2 - \alpha\frac{x}{2}}{\beta} + \mathcal{O}(\frac{1}{\beta^2})\right] ,$$

$$W_{\alpha,\beta}(x) = \frac{\Gamma(2\beta)}{\Gamma(\beta+\frac{1}{2}-\alpha)} x^{-\beta+\frac{1}{2}}\left[1 - \frac{\frac{1}{4}(\frac{x}{2})^2 - \alpha\frac{x}{2}}{\beta} + \mathcal{O}(\frac{1}{\beta^2})\right] \tag{A.4}$$

as $\beta \to \infty$. From these expressions, we obtain the asymptotic forms of the Green's functions for $|\kappa| \to \infty$. We list the cases for positive and negative subscripts separately.

$\kappa > 0$

$$G_\kappa^{11}(ry,y,z) = \frac{r^{\kappa-1}}{2\kappa y^2}[\gamma + (z+1)ry + \mathcal{O}(\tfrac{1}{\kappa})] ,$$

$$G_\kappa^{12}(ry,y,z) = \frac{r^{\kappa-1}}{2\kappa y^2}[\mathcal{O}(\tfrac{1}{\kappa})] ,$$

$$G_\kappa^{21}(ry,y,z) = \frac{r^{\kappa-1}}{2\kappa y^2}[2\kappa - \gamma^2 \ell n\, r + 2\gamma z(1-r)y - \tfrac{1}{2}(1-r^2)c^2y^2 + \mathcal{O}(\tfrac{1}{\kappa})] ,$$

$$G_\kappa^{22}(ry,y,z) = \frac{r^{\kappa-1}}{2\kappa y^2}[\gamma + (z-1)y + \mathcal{O}(\tfrac{1}{\kappa})] ,$$

$$G_{-\kappa}^{11}(ry,y,z) = \frac{r^{\kappa-1}}{2\kappa y^2}[\gamma + (z+1)y + \mathcal{O}(\tfrac{1}{\kappa})] ,$$

$$G_{-\kappa}^{12}(ry,y,z) = -\frac{r^{\kappa-1}}{2\kappa y^2}[2\kappa - \gamma^2 \ell n\, r + 2\gamma z(1-r)y - \tfrac{1}{2}(1-r^2)c^2y^2 + \mathcal{O}(\tfrac{1}{\kappa})] ,$$

Equation (A.5) continued next page

Equation (A.5) continued

$$G_{-\kappa}^{21}(ry,y,z) = \frac{r^{\kappa-1}}{2\kappa y^2}[\mathcal{O}(\tfrac{1}{\kappa})] ,$$

$$G_{-\kappa}^{22}(ry,y,z) = \frac{r^{\kappa-1}}{2\kappa y^2}[\gamma + (z-1)ry + \mathcal{O}(\tfrac{1}{\kappa})] . \qquad (A.5)$$

APPENDIX B

For the computation of the low-energy part, we give the method by which, for a given value of x, $0 < x < 500$, and a given value of L, we evaluate $j_\ell(x)$ and $j'_\ell(x)$ for $0 \le \ell \le L$. To evaluate the Bessel functions, it is convenient to first compute the values of the function

$$r_\ell(x) = \frac{2\ell+3}{x}\,\frac{j_{\ell+1}(x)}{j_\ell(x)} \qquad (B.1)$$

at the point x for ℓ in the range $0 \le \ell < L$. We assume, of course, that x is not a zero of $j_\ell(x)$. From the standard recurrence relation for the Bessel functions, we have

$$r_{\ell-1}(x) = \frac{1}{1 - \frac{x^2}{(2\ell+1)(2\ell+3)}\, r_\ell(x)} . \qquad (B.2)$$

In view of the asymptotic form of $j_\ell(x)$, we have $\lim_{\ell\to\infty} r_\ell(x) = 1$. We compute the $r_\ell(x)$ recursively, with the aid of (B.2), in the direction of decreasing ℓ. To obtain the initial value $r_L(x)$, we use

a variation of the method of J. C. P. Miller [9]. We compute values for the quantities $r_N(x)$, $r_{N-1}(x)$, $r_{N-2}(x),\cdots,r_L(x)$ recursively, with the aid of (B.2), starting with the approximation $r_N(x) \approx 1$. For large enough N, the value obtained for $r_L(x)$ is correct to a predetermined accuracy. The value we use for N is given by

$$N = \max(L,L_0) + [15 + 0.1x] \tag{B.3}$$

where $L_0 = [x]$. The function $[15 + 0.1x]$ was determined empirically by examining the convergence in the sequence of values for $r_{L_0}(x)$ corresponding to a sequence of increasing sample values of N. We chose for N the smallest sample value which leads to a value for $r_{L_0}(x)$ which is correct to approximately 12 significant figures. From the value for $r_L(x)$, values for the $r_\ell(x)$, $0 \le \ell < L$, are calculated. The $j_\ell(x)$ are then computed with the aid of

$$j_0(x) = \frac{\sin x}{x} ,$$

$$j_{\ell+1}(x) = \frac{x}{2\ell + 3} r_\ell(x)\, j_\ell(x) . \tag{B.4}$$

Once the values of the $j_\ell(x)$ are known, the values of $j'_\ell(x)$, $0 \le \ell \le L$, are obtained from $j_\ell(x)$ and $j_{\ell-1}(x)$.

Values for $j_\ell(x)$ and $j'_\ell(x)$ obtained by using the above method were tested by numerically evaluating the following sums:

$$\sum_{\ell=0}^{\infty} (2\ell + 1)\, j_\ell(ry)\, j_\ell(y) = \frac{\sin u}{u} ,$$

$$\sum_{\ell=0}^{\infty} (2\ell + 1)\, \ell(\ell + 1)\, j_\ell(ry)\, j_\ell(y) = 2ry^2 \left(\frac{\sin u}{u^3} - \frac{\cos u}{u^2}\right) ,$$

$$\sum_{\ell=0}^{\infty} (2\ell + 1)\, j'_\ell(ry)\, j_\ell(y) = \frac{\sin u}{u^2} - \frac{\cos u}{u} ,$$

$$\sum_{\ell=0}^{\infty} (2\ell + 1)\, j_\ell(ry)\, j'_\ell(y) = \frac{\cos u}{u} - \frac{\sin u}{u^2} ,$$

$$u = (1 - r)y . \tag{B.5}$$

These sums were evaluated for all combinations of the values $r = 0.2,0.4,\cdots,1.0$ and $y = 0.001,0.005,0.01,0.05,\cdots,500$. In each case, the sum was truncated at $\ell = M$, where M is the smallest number for which the magnitude of the ratio of the Mth term to the sum of the first M terms is less than 10^{-12}. The results are consistent with 12 significant figures being correct in the values for the spherical Bessel functions.

APPENDIX C

We describe here the method used to evaluate the products of spherical Bessel and Hankel functions $j_\ell(x)\, h_\ell^{(1)}(y)$ which arise in the numerical evaluation of ΔE_{HB}. The relevant range for the parameters x, y, and ℓ is given by: $0 < \frac{x}{y} < 1$, $0 < \mathrm{Re}(y) < 200$, $0 < \mathrm{Im}(y) < 20{,}000$, $0 \le \ell \le 20{,}000$. The evaluation is done by a subroutine in which for a given value of x, y, and L, $1 \le L \le 20{,}000$, the set of values $j_\ell(x)\, h_\ell^{(1)}(y)$, $0 \le \ell \le L$, is computed.

It is convenient to first compute the set of values $r_\ell(x)$ defined in Eq. (B.1). We use the method described in Appendix B to compute these values, except that here we replace the number N defined in (B.3) by the number N'

$$N' = \max(L, L_0') + [15 + 0.1\,\mathrm{Re}(x)] , \qquad (C.1)$$

where $L_0' = [|x|]$. This expression for N' was arrived at with the same method as the one described in Appendix B for finding N.

We also compute the set of values $t_\ell(y)$, where

$$t_\ell(y) = \frac{2\ell + 1}{y} \frac{h_\ell^{(1)}(y)}{h_{\ell+1}^{(1)}(y)} , \qquad (C.2)$$

at the point y for ℓ in the range $0 < \ell < L$. We assume $h_{\ell+1}^{(1)}(y) \neq 0$. Because the function $h_\ell^{(1)}(y)$ satisfies the standard recurrence relation, we have

$$t_{\ell+1}(y) = \frac{1}{1 - \frac{y^2}{(2\ell + 1)(2\ell + 3)}\, t_\ell(y)} . \qquad (C.3)$$

We also have $\lim_{\ell \to \infty} t_\ell(y) = 1$. The values $t_\ell(y)$, $0 < \ell < L$, are computed recursively, with (C.4), in the direction of increasing ℓ. The initial value is $t_0(y) = (1 - iy)^{-1}$.

The products $j_\ell(x)\, h_\ell^{(1)}(y)$, $0 \le \ell \le L$, are then computed recursively with the aid of

$$j_0(x)\, h_0^{(1)}(y) = \frac{\sin x}{x} \frac{e^{iy}}{iy} \qquad (C.4)$$

and

$$j_{\ell+1}(x)\, h_{\ell+1}^{(1)}(y) = \frac{2\ell + 1}{2\ell + 3} \frac{x}{y} \frac{r_\ell(x)}{t_\ell(y)}\, j_\ell(x)\, h_\ell^{(1)}(y) . \qquad (C.5)$$

We tested the subroutine which computes the products $j_\ell(x)\, h_\ell^{(1)}(y)$ by numerically evaluating the following sums:

$$\sum_{\ell=0}^{\infty} (2\ell + 1)\, j_\ell(ry)\, h_\ell^{(1)}(y) = \frac{e^v}{v} ,$$

$$\sum_{\ell=0}^{\infty} (2\ell + 1)\, \ell(\ell + 1)\, j_\ell(ry)\, h_\ell^{(1)}(y) = 2r(iy)^2(v^{-3} - v^{-2})e^v , \qquad (C.6)$$

$$v = iy(1 - r) .$$

The evaluation was made for all combinations of the values $\mathrm{Re}(y) = 0.01, 0.02, 0.1, 0.2, \cdots, 100, 200$, $\mathrm{Im}(y) = 0.01, 0.02, 0.1, 0.2, \cdots, 100, 200$, $r = 0.2, 0.4, 0.6, 0.8$, and for all combinations of the values $\mathrm{Re}(y) = 0.01, 0.02, 0.1, 0.2, \cdots, 100, 200$, $\mathrm{Im}(y) = 1000, 2000, 10000, 20000$, and $r = 0.99$. In every case, each sum over ℓ in (C.6) was terminated when the ratio of the last term in the partial sum to the partial sum was less than 10^{-15} in magnitude. The values of the sums agree with the corresponding expressions on the right side in (C.6) to more than 11 significant figures.

APPENDIX D

The method given here for numerically evaluating the radial Green's functions $G_\kappa(x_2, x_1, z)$ is valid for the range of parameters involved in the computation of the low-energy part: $|\kappa| < 500$, $0 < x_2 < x_1 < 250$, and $0 < z < E_1$, where E_1 is the $1S_{\frac{1}{2}}$ bound-state energy. We refer to Eqs. (A.16) and (A.17) of I in which the radial Green's functions are given in terms of Whittaker functions and gamma functions.

The evaluation of $M_{\nu\pm\frac{1}{2},\lambda}(2cx_2)$ is done by evaluating the standard series expansion [10], which is conveniently expressed in the form

$$M_{\alpha,\beta}(x) = x^{\beta+\frac{1}{2}} e^{-\frac{1}{2}x} \sum_{n=0}^{\infty} T(n) \qquad (D.1)$$

where

$$T(0) = 1 \ ,$$

$$T(n+1) = \frac{(n + \beta + \frac{1}{2} - \alpha)x}{(n + 2\beta + 1)(n + 1)} T(n) \ . \qquad (D.2)$$

In our case, the parameters in (D.1) and (D.2) obey the restrictions $-\frac{1}{2} < \alpha < \frac{3}{2}$, $0 < \beta < 500$, $0 < x < 500$, and $\beta + \frac{1}{2} - \alpha > 0$. The terms in the sum in (D.1), which are all non-negative, are easily computed numerically with the aid of (D.2). If the first N terms are used to approximate the sum, the error is estimated by

$$\sum_{n=N+1}^{\infty} T(n) < \frac{N+2}{N+2-x} T(N+1) \quad \text{for } N + 2 > x \ . \qquad (D.3)$$

Terms in (D.1) are summed until the relative error, as determined by (D.3), is $<10^{-12}$. The number of terms necessary is not excessive, because for $N > x$, $T(N)$ approaches zero rapidly as N increases.

We next consider the evaluation of $W_{\alpha,\beta}(x)$. The range for the variables is the same as for $M_{\alpha,\beta}(x)$. Two methods of evaluation are used; the choice of method depends on the magnitude of x.

For $x > 30$, we use the large-x asymptotic expansion [10]

$$W_{\alpha,\beta}(x) = x^{\alpha} e^{-\frac{1}{2}x} \left(\sum_{n=0}^{N} T'(n) + E_N \right) \qquad (D.4)$$

where

$$T'(0) = 1 \ , \tag{D.5}$$

$$T'(n+1) = \frac{(n+\beta+\frac{1}{2}-\alpha)(\beta-\frac{1}{2}+\alpha-n)}{(n+1)x}\,T'(n) \ .$$

We employ the estimate

$$|E_N| \le |T'(N+1)| \qquad \text{for } N+1 > \beta-\tfrac{1}{2}+\alpha \ . \tag{D.6}$$

The value of $W_{\alpha,\beta}(x)$ is then obtained by performing the sum in (D.4). The value for N is determined by requiring that $N+1 > \beta-\frac{1}{2}+\alpha$, and that the ratio of the error, as given by (D.6), to the value of the sum be less than 10^{-12} in magnitude. For $x > 30$, we find empirically that such an accuracy can always be achieved.

For $x \le 30$, $W_{\alpha,\beta}(x)$ is computed with the aid of the standard formula in which $W_{\alpha,\beta}(x)$ is expressed as a linear combination of $M_{\alpha,-\beta}(x)$ and $M_{\alpha,\beta}(x)$ [10]. That formula is expressed, for $2\beta \neq$ integer, as

$$W_{\alpha,\beta}(x) = \frac{\Gamma(2\beta)}{\Gamma(\beta+\frac{1}{2}-\alpha)}\,x^{\frac{1}{2}-\beta}\,e^{-\frac{1}{2}x}(U+\eta S) \ , \tag{D.7}$$

where

$$\eta = -x^{2\beta}\,\frac{\sin[\pi(\beta+\frac{1}{2}+\alpha)]}{\sin(\pi 2\beta)}\,\frac{\Gamma(\beta+\frac{1}{2}-\alpha)\,\Gamma(\beta+\frac{1}{2}+\alpha)}{\Gamma(2\beta)\,\Gamma(2\beta+1)} \ ; \tag{D.8}$$

the terms U and S are given by

$$U = \sum_{n=0}^{\infty} V(n) \ ; \qquad S = \sum_{n=0}^{\infty} T(n) \ , \tag{D.9}$$

where

$$V(0) = 1 \ ,$$

$$V(n+1) = \frac{(n-\beta+\frac{1}{2}-\alpha)x}{(n-2\beta+1)(n+1)}\,V(n) \ , \tag{D.10}$$

and where $T(n)$ is defined in (D.2). The error which results from truncating the first sum in (D.9) after N terms is

$$\left|\sum_{n=N+1}^{\infty} V(n)\right| < \frac{N+2}{N+2-\theta x}|V(N+1)| \tag{D.11}$$

for $N+2 > \max(2\beta+1, \theta x)$, where

$$\theta = \max\left(\frac{(N+1-\beta+\frac{1}{2}-\alpha)}{(N+1-2\beta+1)}, 1\right) \ . \tag{D.12}$$

Guided by the estimates in (D.11) and (D.3), one can evaluate the individual terms U and S numerically to a preassigned precision. However, the expression in (D.7) is numerically unsafe when x is large and β is small. This can be seen by considering the large-x asymptotic forms for $M_{\alpha,\beta}(x)$ and $W_{\alpha,\beta}(x)$ given in Eq. (A.2). We find that for $x \to \infty$

$$\frac{U+\eta S}{|U|+|\eta S|} \sim \left|\frac{\sin(2\pi\beta)}{2\pi}\,\Gamma(\beta+\tfrac{1}{2}-\alpha)\,\Gamma(-\beta+\tfrac{1}{2}-\alpha)\right| x^{2\alpha}\,e^{-x} \ . \tag{D.13}$$

Hence in the worst case, which occurs when $x = 30$, the sum is roughly e^{-30} times the individual terms, which corresponds to a loss of approximately 13 significant figures. We have studied this cancellation numerically, and find that by using double precision arithmetic, which gives approximately 27 significant figure accuracy, we can achieve better than 12 significant figure accuracy in the evaluation of the sum $U + \eta S$. In evaluating $W_{\alpha,\beta}(x)$, we truncate the first sum over n in (D.9) when the magnitude of the ratio of the remainder of the sum to the partial sum is less than 10^{-28}. We then truncate the second sum over n in (D.9) at $n = N$ when the magnitude of the ratio

$$\eta \sum_{m=N+1}^{\infty} T(m) \left[U + \eta \sum_{n=0}^{N} T(n) \right]^{-1} \tag{D.14}$$

is less than 10^{-12}.

For $x = 30$, we compared the two values obtained for $W_{\alpha,\beta}(x)$ using the two methods described above. The comparison was made for various combinations of the remaining parameters. In all cases, the two values agree to approximately 12 significant figures.

The method that we use for evaluating the gamma function is described in Appendix F.

We note that care is required in handling potentially very large or very small quantities in the evaluation of the radial Green's functions. Quantities such as x^{β} or $\Gamma(2\beta)$ can be greater than 10^{1000} for the range of values of x and β under consideration. Such magnitudes are out of the range for real constants in the computer. The allowed range is given by $10^{-294} < |R| < 10^{322}$. In order to

avoid this problem, we compute the logarithm of quantities with extreme magnitudes. We find that when all such factors have been combined, the result is of moderate magnitude and can be safely exponentiated. For the parameters which occur in the low-energy evaluation of the radial Green's functions, the range of magnitude of the terms in the sums in (D.1), (D.4), and (D.9) is within the allowed limits.

As a check that the numerical evaluation of the radial Green's functions was programmed correctly, we computed the expectation value of the Dirac Green's function in various bound states. We note the identity

$$\begin{aligned} 1 &= (E_n - z)\langle G(z)\rangle \\ &= (E_n - z)\int_0^{\infty} dx_2 \int_0^{\infty} dx_1 x_2^2 x_1^2 \sum_{i,j=1}^{2} f_i(x_2) G_{\kappa_n}^{ij}(x_2, x_1, z) f_j(x_1), \end{aligned} \tag{D.15}$$

where κ_n is the angular quantum number of the bound state ψ_n. The integrals in (D.15) were evaluated numerically with essentially the same techniques as those described in Sec. II. The evaluation was made for all states with principal quantum number 1 or 2, for nuclear charges of 10 and 110, and for energies $z = 0.1E_1, 0.2E_1, \cdots, 0.9E_1$. In all cases, the error in the result is less than 10^{-11}.

APPENDIX E

In this appendix, we give the method used to evaluate the Coulomb radial Green's functions $G_\kappa(x_2,x_1,z)$ for the range of parameters encountered in the numerical evaluation of ΔE_{HB}. The range is $|\kappa| < 20{,}000$, $0 < x_2 < x_1 < 200$, $\mathrm{Re}(z) = 0$, $0 < \mathrm{Im}(z) < 100$.

We first consider the evaluation of $M_{\alpha,\beta}(x)$ for the corresponding range of variables: $\mathrm{Re}(\alpha) = \pm\frac{1}{2}$, $0 < \mathrm{Im}(\alpha) < 1$, $0 < \beta < 20{,}000$, $0 < x < 40{,}000$. Two methods of evaluation are used. The choice of method depends on the relative magnitude of x and β. For $x < 20\,\beta^{\frac{1}{2}}$, we employ the power series for $M_{\alpha,\beta}(x)$ obtained by expanding the exponential function in the integral representation

$$M_{\alpha,\beta}(x) = \frac{\Gamma(1+2\beta)}{\Gamma(\beta+\frac{1}{2}-\alpha)\,\Gamma(\beta+\frac{1}{2}+\alpha)}\,x^{\beta+\frac{1}{2}}\int_0^1 dt\; t^{\beta-\frac{1}{2}-\alpha}(1-t)^{\beta-\frac{1}{2}+\alpha} \times e^{(t-\frac{1}{2})x} \quad , \tag{E.1}$$

valid for $\mathrm{Re}(\beta+\frac{1}{2}\pm\alpha) > 0$ and $|\arg x| < \pi$, in powers of x. The resulting series is

$$M_{\alpha,\beta}(x) = x^{\beta+\frac{1}{2}}\sum_{n=0}^{\infty} I(n)\,\frac{\left(\frac{x}{2}\right)^n}{n!} \tag{E.2}$$

where

$$I(n) = \frac{\Gamma(1+2\beta)}{\Gamma(\beta+\frac{1}{2}-\alpha)\,\Gamma(\beta+\frac{1}{2}+\alpha)}\int_0^1 dt\; t^{\beta-\frac{1}{2}-\alpha}(1-t)^{\beta-\frac{1}{2}+\alpha} \times (2t-1)^n \quad . \tag{E.3}$$

It is convenient to consider the corresponding expansions

$$M_{\nu-\frac{1}{2},\lambda}(2cx_2) \pm M_{\nu+\frac{1}{2},\lambda}(2cx_2) = (2cx_2)^{\lambda+\frac{1}{2}}\sum_{n=0}^{N} I_\pm(n)\,\frac{(cx_2)^n}{n!} + E_\pm(N) \tag{E.4}$$

where ν, λ, and c are the parameters which appear in (A.16) of I, and where $E_\pm(N)$ are the remainders. The functions $I_\pm$ satisfy the equations

$$I_+(n+1) = I_-(n) - \frac{2\nu}{n+1+2\lambda}\,I_+(n) \quad ,$$
$$I_-(n+1) = \frac{n+1}{n+1+2\lambda}\,I_+(n) \quad . \tag{E.5}$$

These relations together with the initial values $I_+(0) = 2$ and $I_-(0) = 0$ provide a simple and safe method for numerically evaluating the series in (E.4). We obtain approximate values for the errors $E_\pm$ in (E.4), which arise from truncating the sum over n at $n = N$, by estimating these errors to lowest order in ν:

$$|E_+(N)| < (2cx_2)^{\lambda+\frac{1}{2}}|I_+(N+1)|\frac{(cx_2)^{N+1}}{(N+1)!}\,\frac{(2\lambda+N+2)(N+3)}{(2\lambda+N+2)(N+3)-(cx_2)^2} \times [1+\mathcal{O}(|\nu|)] \quad , \tag{E.6}$$

valid when N is odd and satisfies $(2\lambda+N+2)(N+3) > (cx_2)^2$;

$$|E_-(N)| < (2cx_2)^{\lambda+\frac{1}{2}}|I_-(N+1)|\frac{(cx_2)^{N+1}}{(N+1)!}\frac{(2\lambda+N+3)(N+2)}{(2\lambda+N+3)(N+2)-(cx_2)^2}$$

$$\times [1 + \mathcal{O}(|\nu|)] , \qquad (E.7)$$

valid when N is even and satisfies $(2\lambda + N + 3)(N + 2) > (cx_2)^2$. In the numerical evaluation of the sums in (E.4), the value of N is taken to be the smallest value for which both the inequality $(2\lambda + N + 3)(N + 2) > (cx_2)^2$ is satisfied and the errors $E_\pm$ corresponding to N and $N - 1$, as estimated in (E.6) and (E.7), are less than 10^{-12} times the corresponding partial sums in magnitude.

The numerical evaluation of $M_{\alpha,\beta}(x)$ for $x \geq 20\beta^{\frac{1}{2}}$ is done with the aid of the expansion in (D.1). In this case, the summation is begun at $n = n_0$, where $n_0 = [(\beta^2 + \frac{1}{4}x^2)^{\frac{1}{2}} + \frac{1}{2}x - \beta]$ is approximately the value of n for which the magnitude of $T(n)$, defined in (D.2), has its maximum value. The sum is evaluated by summing terms $\bar{T}(n)$ normalized so that $T(n) = T(n_0)\bar{T}(n)$:

$$M_{\alpha,\beta}(x) = x^{\beta+\frac{1}{2}} e^{-\frac{1}{2}x} T(n_0) \sum_{n=0}^{\infty} \bar{T}(n) . \qquad (E.8)$$

The summation is performed first in the direction of increasing n until $n = N_1$, and then in the direction of decreasing n until $n = N_2$. The values N_1 and N_2 are determined by evaluating the error which would result from truncating the sum over n as each term is added and continuing the summation until the relative magnitude of the error from truncating the sum is less than 10^{-11}. The errors are estimated by

$$\left|\sum_{n=N_1+1}^{\infty} \bar{T}(n)\right| < \frac{1}{1-\theta}|\bar{T}(N_1+1)| , \qquad (E.9)$$

$$\theta = \left|\frac{(N_1 + \frac{3}{2} + \beta - \alpha)x}{(N_1 + 2 + 2\beta)(N_1 + 2)}\right| ,$$

valid for N_1 large enough that $\theta < 1$, and by

$$\left|\sum_{n=0}^{N_2-1} \bar{T}(n)\right| < N_2|\bar{T}(N_2 - 1)| \qquad (E.10)$$

valid for N_2 smaller than the value of n for which $|\bar{T}(n)|$ is at the maximum. From the coefficient of the sum in (E.8), we store separately in the computer the complex logarithm of

$$\frac{\Gamma(n_0 + \beta + \frac{1}{2} - \alpha)}{\Gamma\left(n_0 + \beta + \frac{1}{2} - \mathrm{Re}(\alpha)\right)} \frac{\Gamma\left(\beta + \frac{1}{2} - \mathrm{Re}(\alpha)\right)}{\Gamma(\beta + \frac{1}{2} - \alpha)} \qquad (E.11)$$

and the double precision logarithm of

$$\frac{\Gamma\left(n_0 + \beta + \frac{1}{2} - \mathrm{Re}(\alpha)\right)\Gamma(2\beta+1)x^{n_0+\beta+\frac{1}{2}}}{\Gamma\left(\beta + \frac{1}{2} - \mathrm{Re}(\alpha)\right)\Gamma(n_0 + 2\beta + 1)\cdot\Gamma(n_0 + 1)} e^{-\frac{1}{2}x} . \qquad (E.12)$$

Storing the double precision logarithm of (E.12) is necessary because of the loss of significant figures which occurs when the logarithm of a quantity with a very large magnitude is added to the logarithm of a quantity with a very small magnitude. This loss can occur when the various factors in the radial Green's functions are combined.

As a test of the programming of the two methods of evaluation of $M_{\alpha,\beta}(x)$ given above, we compared the two values obtained for this function with these methods for $x = 20\beta^{\frac{1}{2}}$ and α and β given a large number of sample values which cover the range for these parameters relevant to the evaluation of ΔE_{HB}. In all cases, the relative magnitude of the difference of the two values was less than 10^{-11}.

In the numerical evaluation of $W_{\alpha,\beta}(x)$, the choice of method of evaluation depends, as in Appendix D, on whether x is less than or greater than 30. The two methods used here are basically the same as those described in Appendix D, except for some modifications necessary to accommodate the large range of parameters and complex numbers which occur here.

For $x \geq 30$, we evaluate $W_{\alpha,\beta}(x)$ with the aid of the asymptotic expansion given by Eqs. (D.4) and (D.5). The summation over n in (D.4) is begun at $n = n_0'$, where $n_0' = [(\beta^2 + \frac{1}{4}x^2)^{\frac{1}{2}} - \frac{1}{2}x]$ is approximately the value of n for which the magnitude of $T'(n)$ is at its first relative maximum encountered as the value of n increases from zero. Normalized terms $\bar{T}'(n) = T'(n)/T'(n_0')$ are employed in evaluating the sum:

$$W_{\alpha,\beta}(x) = x^{\alpha} e^{-\frac{1}{2}x} T'(n_0)\left(\sum_{n=0}^{N_2'} \bar{T}'(n) + \bar{E}_{N_2'}\right) . \qquad (E.13)$$

We sum first in the direction of decreasing n until $n = N_1'$ and then in the direction of increasing n until $n = N_2'$. In each direction, the summation is terminated when the magnitude of the ratio of the error to the partial sum is less than 10^{-11}. We employ the error estimates

$$\left|\sum_{n=0}^{N_1'-1} \bar{T}'(n)\right| \leq N_1'|\bar{T}'(N_1' - 1)| \qquad (E.14)$$

valid for N_1' smaller than the value n for which $|\bar{T}'(n)|$ is at its first relative maximum, and

$$|\bar{E}_{N_2'}| \leq \left[M + \frac{1}{|\Gamma(1 - i\mathrm{Im}(\alpha))|}\right] |\bar{T}'(N_2' + 1)| ,$$
$$M = \max\left(0, \left[\mathrm{Re}\left(\beta - \tfrac{1}{2} + \alpha - N_2'\right)\right]\right) \qquad (E.15)$$

valid for N_2' larger than the value n for which $\bar{T}'(n)$ is at its first relative maximum. The coefficient of the sum in (E.13) is factorized into a complex factor with magnitude of order 1 whose complex logarithm is stored, and a real factor whose double precision logarithm is stored, in analogy with the separation shown in (E.11) and (E.12).

For $x \leq 30$, we employ the method described in Appendix D, beginning with Eq. (D.7), to evaluate $W_{\alpha,\beta}(x)$. It is necessary to have double precision accuracy in that method. This is accomplished here by explicitly programming the complex arithmetic operations in terms of separate double precision real and imaginary parts for the variables involved. The term S, which appears in (D.7), is evaluated with the aid of (D.2) and (D.9). An estimate for the error which results from truncating the sum over n at a finite value N is easily obtained with the appropriate modification of the discussion of (E.8). The term U, which appears in (D.7), is evaluated with the

aid of (D.9) and (D.10). The error which results from truncating the relevant sum over n in (D.9) at $n = N$ is estimated by

$$\left| \sum_{n=N+1}^{\infty} V(n) \right| < \frac{1}{1-\theta} |V(N+1)| \quad , \tag{E.16}$$

$$\theta = \left| \frac{(N - \beta + \frac{3}{2} - \alpha)x}{(N - 2\beta + 2)(N + 2)} \right|$$

valid for $N + 1 \geq \max\left(2, \left[\beta + \frac{1}{2}x + \left(\beta^2 + \frac{1}{4}x^2 + x\right)^{\frac{1}{2}}\right]\right)$.

To evaluate $W_{\alpha,\beta}(x)$ with the preceding method, we need the full double precision accuracy for certain combinations of the parameters. The worst case, where the full accuracy is required, is for $|\kappa| = 1$ and x near 30. We explored other regions in the parameter space by examining the numerical behavior of the series for sample values of the parameters. On the basis of this study, we found that some time-saving modifications in the method of evaluation could be made in certain regions of the parameter space. For $\beta < 40$ and $x \leq \frac{3}{2}(\beta - 6)$, single precision arithmetic is used. For $\beta \geq 40$, the contribution of the term ηS in (D.7) is negligible and the term U is evaluated with single precision arithmetic; in this case, the contribution to the first sum in (D.9) from terms with $n > \beta$ is negligible.

To check the programming of the two methods of evaluation of $W_{\alpha,\beta}(x)$ described above, we compared the two values obtained with the two methods for $x = 30$ and sample values for the remaining parameters. This was done for a large number of sample values, and in all cases, the agreement between the two values for $W_{\alpha,\beta}(x)$ was satisfactory.

We now briefly describe the method used to evaluate the free radial Green's functions $F_\kappa(x_2, x_1, z)$ for the range of parameters given in the beginning of this appendix. The free Green's functions are given in terms of spherical Bessel and Hankel functions of imaginary argument in (A.20) of I.

We first consider the evaluation of $j_\ell(ix)$. We employ the power series

$$j_\ell(ix) = \left(\frac{ix}{2}\right)^\ell \sum_{n=0}^{\infty} \frac{\Gamma(\frac{3}{2})}{\Gamma(n + \ell + \frac{3}{2})} \frac{1}{n!} \left(\frac{x}{2}\right)^{2n} \quad . \tag{E.17}$$

The summation over n in (E.17) is begun at $n = n_0$, where $n_0 = \left[\frac{1}{2}(\ell^2 + x^2)^{\frac{1}{2}} - \frac{1}{2}\ell\right]$, which is near the value of n for which the magnitude of the terms in the sum is the maximum. The summation is performed first in the direction of decreasing n, and then in the direction of increasing n from n_0. In each case, we terminate the sum when the magnitude of the ratio of the remainder to the partial sum is less than 10^{-11}. Estimates for the remainders are easily obtained as in the Coulomb case. The sum over n is normalized by extracting the n_0th term as an overall factor.

To evaluate $h_\ell^{(1)}(ix)$, we employ the series

$$h_\ell^{(1)}(ix) = -(2ix)^{-\ell} \frac{e^{-x}}{x} \sum_{n=0}^{\ell} \frac{\Gamma(2\ell + 1 - n)(2x)^n}{\Gamma(\ell - n + 1)\,\Gamma(n + 1)} \quad . \tag{E.18}$$

The method we use for evaluating the sum is the analog of that used in the evaluation of $j_\ell(ix)$; in this case we have $n_0 = [\ell + x - (\ell^2 + x^2)^{\frac{1}{2}}]$.

As a check on the programming of the Coulomb radial Green's function algorithm, we numerically evaluated expectation values of the Green's function. The relevant formula appears in (D.15). The evaluation was made for the state with $n = 2$, $\kappa = -2$, where $Z = 110$, and for the state with $n = 2$, $\kappa = -1$, where $Z = 10$. In both cases, evaluations were made for values of the energy given by $z = iu$, where $u = 1,51,101,151$, and 201. In all cases, the result was correct to at least 11 significant figures. As a check on the programming of the free radial Green's function algorithm, we numerically performed the sum over κ in the 1,1 element of the free Green's function, in the form corresponding to (A.14) of I, for the case $\hat{x}_2 = \hat{x}_1$. The sum over κ was terminated at $|\kappa| = N$ when the magnitude of the ratio of the Nth term of the sum to the partial sum was less than 10^{-15}. The result was compared numerically to the value for the sum obtained from the expression in (A.21) of I. The comparison was made for all combinations of the values $x_2/x_1 = 0.2,0.8$, $x_1 = 0.1,1,10$, and $z = 0.79i$, and for the values $x_2/x_1 = 0.95$, $x_1 = 0.1,1,10$, and $z = 197i$. In all cases, there was agreement to at least 12 significant figures. Further checks were performed on both the Coulomb and free radial Green's function programs. We checked numerically that the functions satisfied the appropriate differential equation. We also examined numerically the asymptotic behavior of the functions in the limit $|\kappa| \to \infty$, with the remaining parameters fixed, and in the limit $x_1 \to \infty$, with x_2/x_1 and the remaining parameters fixed. The asymptotic values were compared with the values obtained from Eqs. (A.3) and (A.5). The results are in satisfactory agreement.

APPENDIX F

Our numerical evaluation of the gamma function is based on Stirling's asymptotic series [10]

$$\ell n\, \Gamma(y) = (y - \tfrac{1}{2})\, \ell n\, y - y + \tfrac{1}{2}\, \ell n(2\pi) + \frac{1}{12y} - \frac{1}{360y^3} + \frac{1}{1260y^5} - \frac{1}{1680y^7} + \frac{1}{1188y^9} - \frac{691}{360360y^{11}} + \frac{1}{156y^{13}} - \frac{3617}{122400y^{15}} + R \quad . \tag{F.1}$$

For y positive real, we have [10]

$$0 < R < \frac{43867}{244188}\,\frac{1}{y^{17}} \quad . \tag{F.2}$$

Two sets of values which we employ are

$$\begin{aligned} &0 < R < 10^{-14} \qquad \text{for} \quad y > 7 \ , \\ &0 < R < 10^{-28} \qquad \text{for} \quad y > 46 \ . \end{aligned} \tag{F.3}$$

The second set of values is relevant to double precision evaluation of the gamma function. From the relations in (F.3), it follows that for sufficiently large y, we obtain an accurate value for the gamma function by evaluating the series in (F.1). To evaluate the gamma function of argument x, where x is too small to satisfy the relevant condition in (F.3), we take advantage of the relation

$$\Gamma(x) = \left\{ \prod_{i=0}^{n-1} \frac{1}{(x + i)} \right\} \Gamma(x + n) \quad . \tag{F.4}$$

In (F.4), we choose n large enough that $y = x + n$ is greater than the appropriate number in (F.3). We then evaluate $\Gamma(y)$ with the series in (F.1), and obtain $\Gamma(x)$ with the aid of (F.4). The relative error in this value for $\Gamma(x)$ is then just R.

In the case where y is complex and satisfies the condition $|\arg y| \leq \frac{1}{4}\pi$, we have the slightly weaker bound on the remainder R in (F.1) [10]:

$$|R| < \frac{43867}{244188} \frac{1}{|y|^{17}} . \qquad (F.5)$$

Thus, for $\max\left(7, \mathrm{Re}(x)\right) \geq |\mathrm{Im}(x)|$, we employ the preceding method to evaluate $\Gamma(x)$, choosing n in (F.4) large enough that $\mathrm{Re}(x + n) > 7$.

REFERENCES

1. P. J. Mohr, Lawrence Berkeley Laboratory report LBL-2153, hereafter referred to as I.
2. A. H. Stroud and Don Secrest, "Gaussian Quadrature Formulas," Prentice-Hall, Englewood Cliffs, 1966.
3. G. W. Erickson, Phys. Rev. Letters 27 (1971) 780.
4. A. M. Desiderio and W R. Johnson, Phys. Rev. A3 (1971) 1267.
5. G. E. Brown and D. F. Mayers, Proc. Roy. Soc. (London) A251 (1959) 105.
6. G. W. Erickson and D. R. Yennie, Ann. Phys. (N.Y.) 35 (1965) 271, 447.
7. Such behavior is consistent with the findings in Zh. Eksp. Teor. Fiz. 59 (1970) 2165 [Sov. Phys.-JETP 32 (1971) 1171].
8. W. Magnus, F. Oberhettinger, and R. P. Soni, "Formulas and Theorems for the Special Functions of Mathematical Physics," third edition, Springer-Verlag, New York, 1966.
9. There are numerous variations of Miller's method in the literature. A relevant discussion appears in W. Gautschi, SIAM Rev. 9 (1967) 24.
10. E. T. Whittaker and G. N. Watson, "A Course of Modern Analysis," Cambridge University Press, Cambridge, 1927.

FIGURE CAPTIONS

Fig. 1. In this graph, we have plotted $\log_{10}|T_\kappa(r,y,t,\gamma)|$ as a function of κ, for various values of r, y, t, and γ. The vertical line on each curve gives the value, on the same scale as κ, of the smaller argument of the Bessel functions in (2.4).

Fig. 2. The points in this graph are the calculated values of $f_L(Z\alpha) - \frac{4}{3}\ell n(Z\alpha)^{-2}$ for $Z = 10$, 20, 30, 40, and 50. The point at $Z = 0$ is the limit as $Z\alpha \to 0$, of the same function and is obtained by an independent method.

Fig. 3. Numerically calculated values for $f_{HB}(Z\alpha)$ for $Z = 10$, 20, 30, 40, and 50 and the value of the limit point $f_{HB}(0)$ which is obtained analytically.

Fig. 4. Values for the function $F(Z\alpha)$ obtained in this calculation and values for $F(Z\alpha)$ based on the results of Erickson [3], Desiderio and Johnson [4], and Brown and Mayers [5]. The curve with the error estimates is based on the graph given in Ref. 3. According to Desiderio and Johnson, there is an error in algebra in the work leading to the result of Brown and Mayers.

Fig. 5. Calculated values for $G(Z\alpha)$. The error limits on the point at $Z = 10$ correspond to the error limits of $F(Z\alpha)$ at $Z = 10$. The dashed line shows the function $G_A(Z\alpha)$ fitted to $G(Z\alpha)$ at $Z = 10$, 20, and 30.

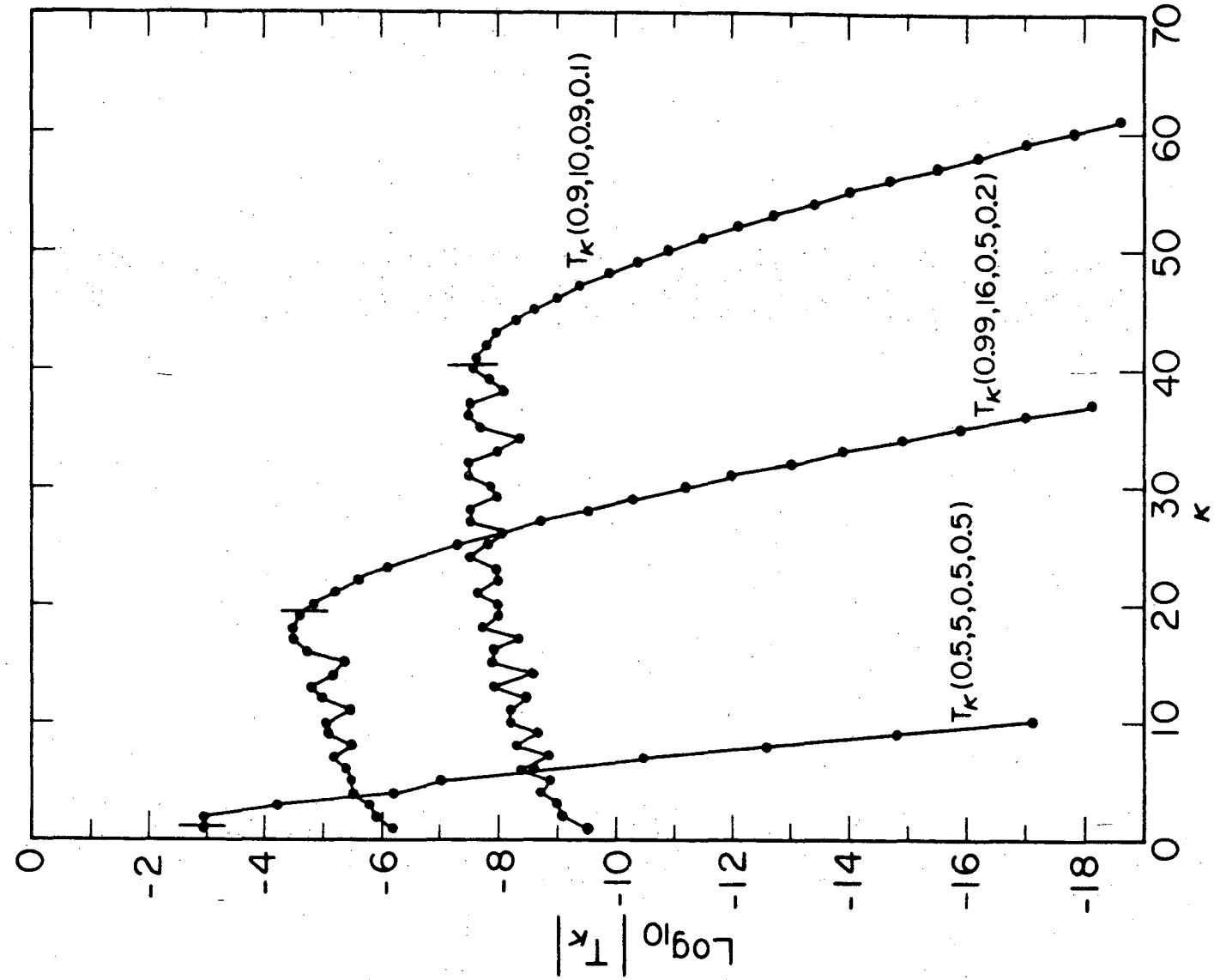

XBL735-2934

Fig. 1

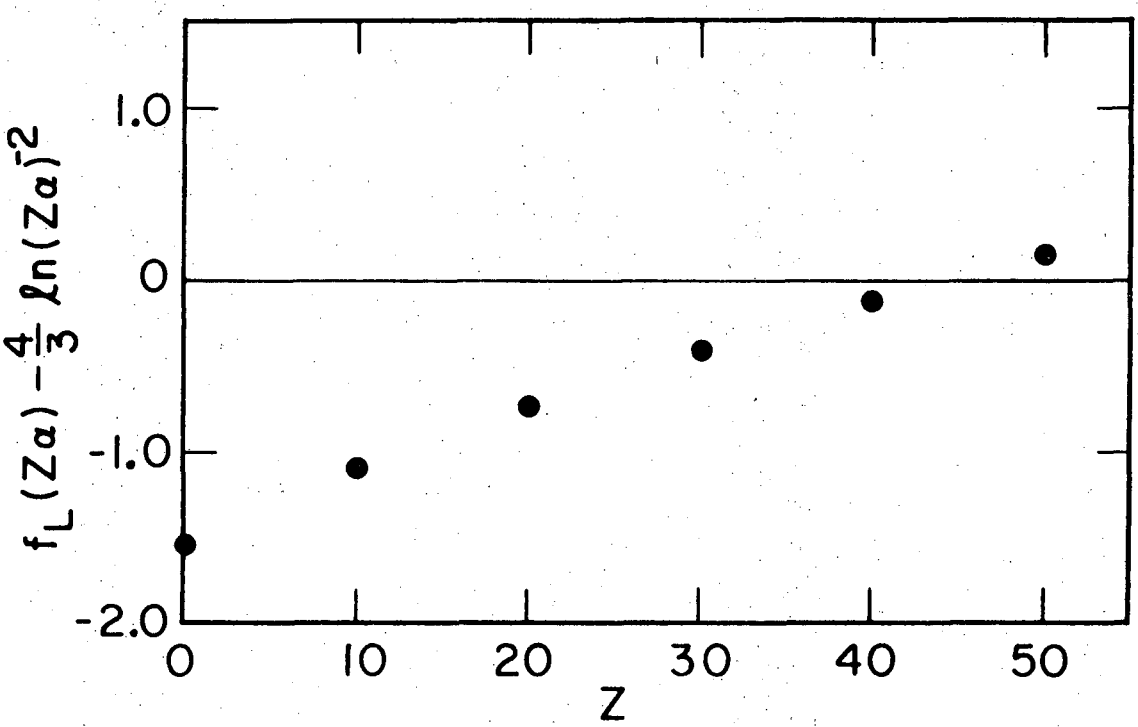
$f_L(Z\alpha) - \frac{4}{3} \ln(Z\alpha)^2$
1.0
0
-1.0
-2.0
0
10
20
30
40
50
Z
XBL 735 - 2933

Fig. 2

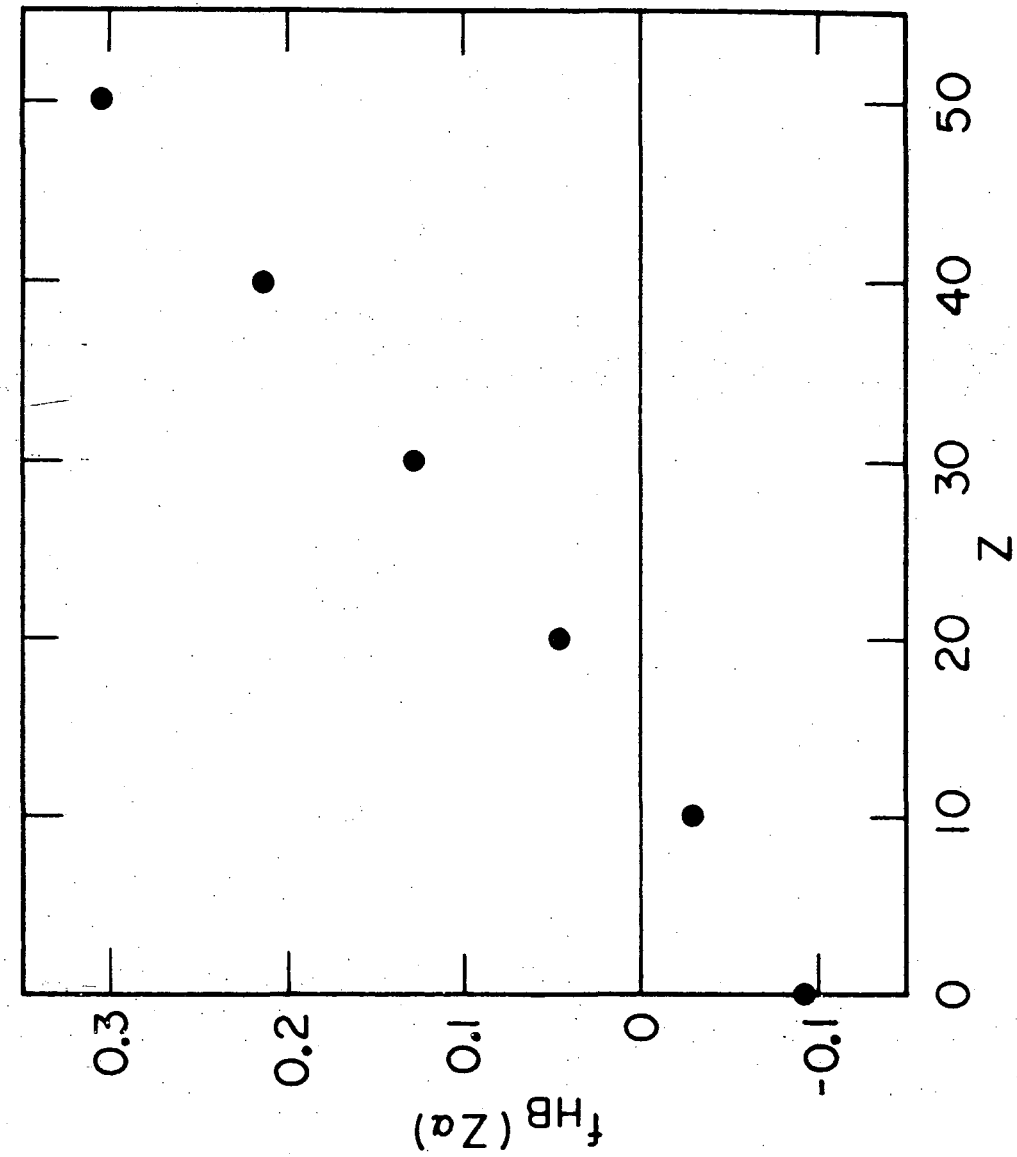

XBL735-2932

Fig. 3

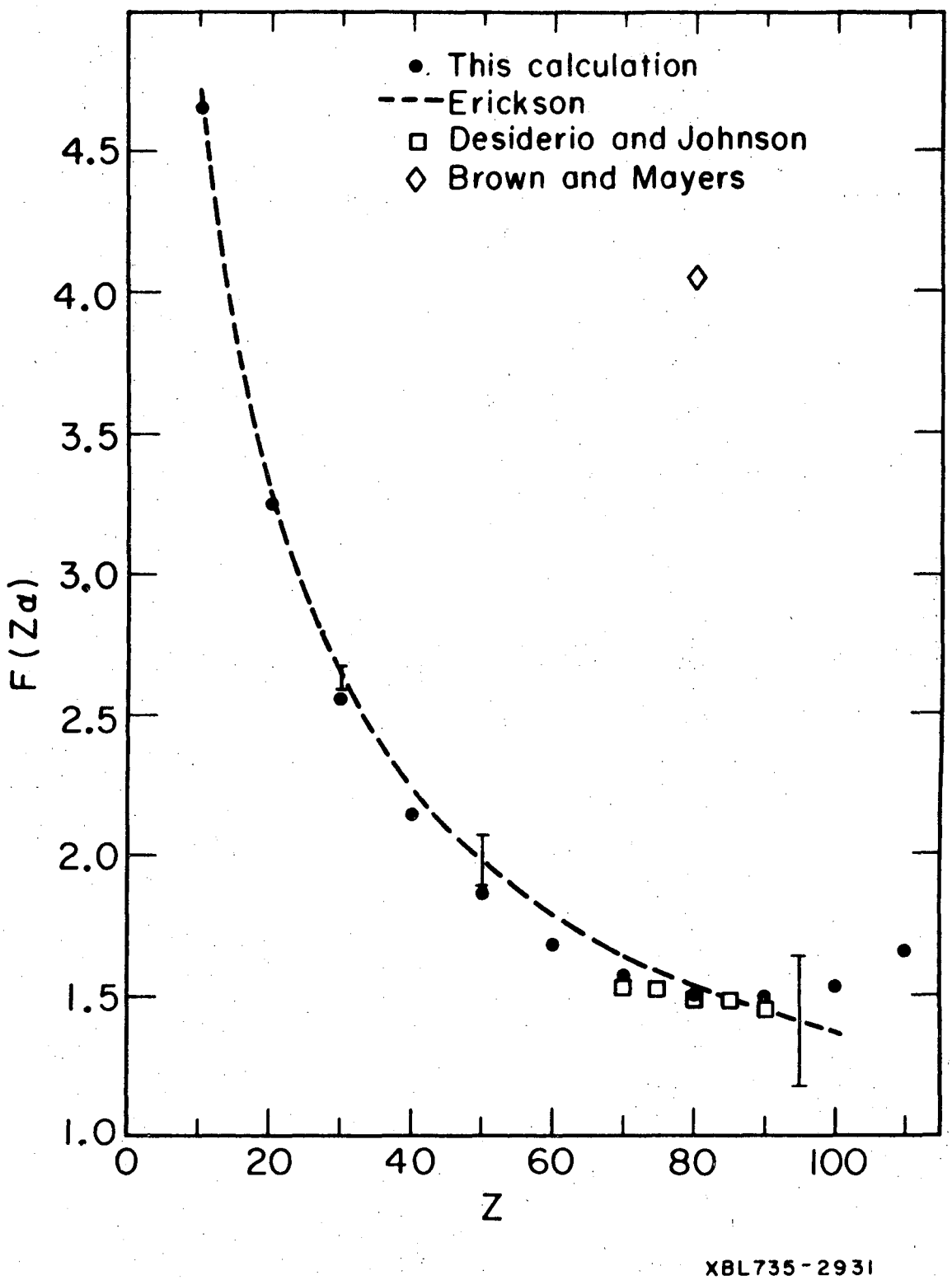
This calculation
Erickson
Desiderio and Johnson
Brown and Mayers
F(Zα)
Z
4.5
4.0
3.5
3.0
2.5
2.0
1.5
1.0
0
20
40
60
80
100
XBL735-2931

Fig. 4

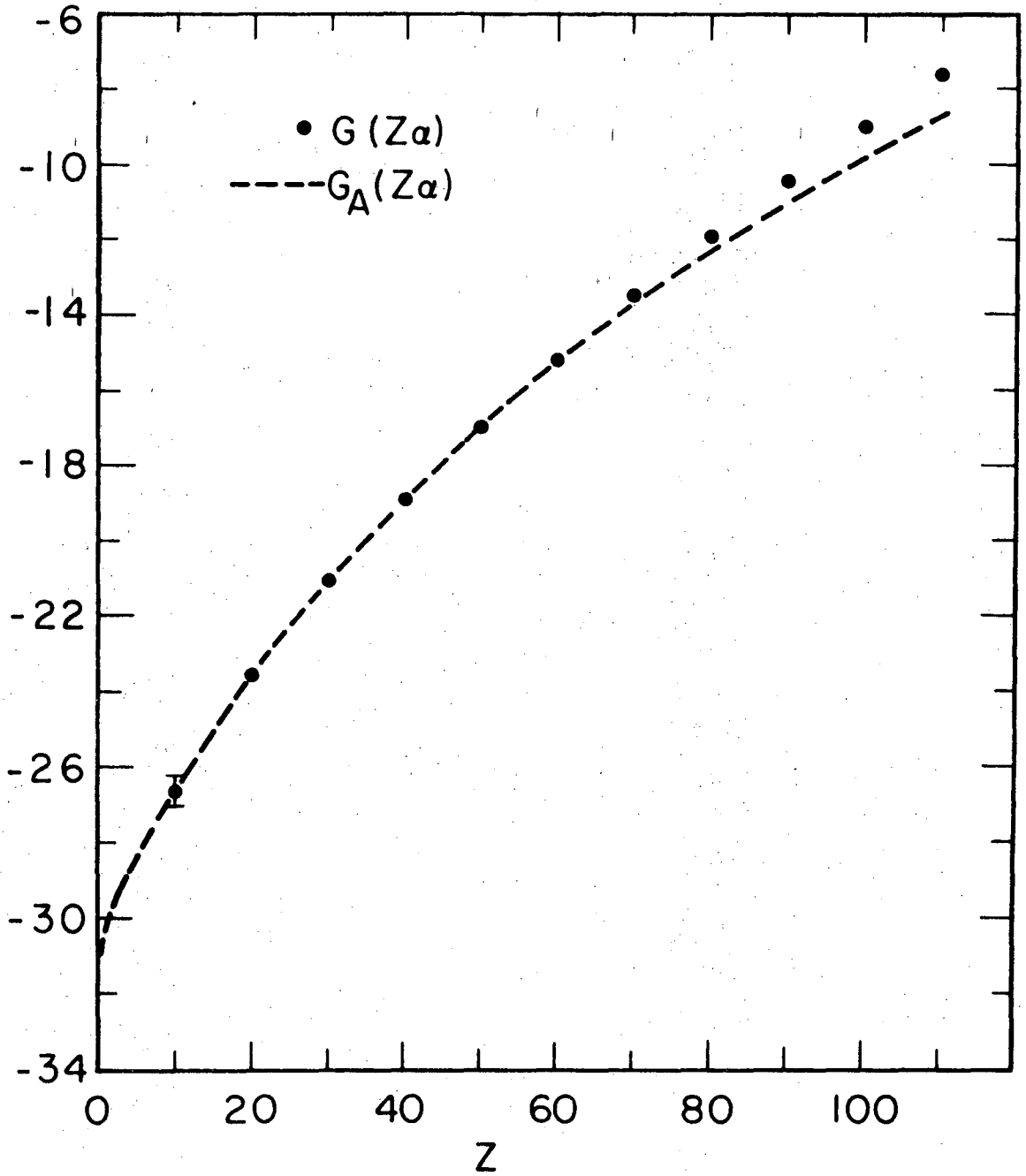

Fig. 5

TECHNICAL INFORMATION DIVISION
LAWRENCE BERKELEY LABORATORY
UNIVERSITY OF CALIFORNIA
BERKELEY, CALIFORNIA 94720